STUDY OF ENZYMES REQUIRED FOR THE SYNTHESIS OF THE ENTEROBACTERIAL COMMON ANTIGEN *IN VITRO*

by

Cassidy Lynn Oliverio

A thesis submitted to the faculty of
The University of North Carolina at Charlotte
in partial fulfillment of the requirements
for the degree of Master of Science in
Biology

Charlotte

2021

Approved by:

_____
Dr. Jerry Troutman

_____
Dr. Richard Chi

_____
Dr. Andrew Truman

ABSTRACT

CASSIDY LYNN OLIVERIO. Study of Enzymes Required for The Synthesis of The Enterobacterial Common Antigen *in Vitro*
(Under the direction of DR. JERRY TROUTMAN)

In recent years, the Center for Disease Control (CDC) has highlighted many bacteria as being either serious or urgent threats in terms of antibiotic resistance such as *Salmonella enterica*, *Klebsiella,* and *Shigella*. These bacteria are all members of the bacterial family *Enterobacteriaceae*, and therefore all produce a complex oligosaccharide known as the Enterobacterial Common Antigen (ECA). Consisting of a polymerized trisaccharide repeat, the ECA can be presented either on the outer membrane of the bacteria, or within the periplasmic space. Although discovered in 1963, the exact function of the ECA has remained unknown. Some research points to involvement in virulence of *Salmonella*, and more recently, the regulation of membrane permeability. The two enzymes involved in the biosynthesis pathway that are focused on in this work include the acetyltransferase WecD and the ECA polymerase WzyE. High performance liquid chromatography (HPLC) was utilized to detect the production of the WecD reaction product, dTDP-Fuc4NAc. After using mass to confirm the product, colorimetric kinetics assays were performed using a 96-well plate and a spectrophotometer and using HPLC. When UDP-Fuc4NH_2 was used as a substrate, turnover was significantly different from that of the dTDP-Fuc4NH_2 reaction at the 30- and 60-minute time points, whereas they were similar at the 120-minute point. We also tested the difference between three constructs of WecD, and found that for most concentrations of substrate, there a significant difference in the rate of reactions at some concentration of AcCoA, however no clear pattern could be determined. When WzyE was incubated with ECA Lipid III for 60 minutes and analyzed via LCMS, a

change in ECA Lipid III levels was observed that differed from that of the control reaction. This suggests that WzyE potentially worked *in vitro* but will require future studies to confirm.

ACKNOWLEDGEMENTS

I would like to thank all those who have guided me along the way and have aided my work with their own expertise. First, I would like to show my gratitude to Claire Gates for getting the groundwork laid out with RffG and WecE and giving me a great starting off point to my project. To Colleen Eade, for training me when I joined the lab; thank you for answering all my silly questions and for helping me begin my journey as a scientist. Thank you to Amanda Reid and Beth Scarbrough, who taught me how to be a proper graduate student and never hesitating to help me. I look up to the both of you, so thank you for being wonderful examples of the type of woman I hope to be someday. Thank you to Kyle Jones, for just being a great friend and a fun person to talk to. Even though we didn't get to know each other very long, thank you to Hailey Houde and Theresa Black for always being supportive when I'm freaking out over everything. And in terms of moral support, I couldn't be more grateful for Matthew Faussett. Thank you for listening to me vent about unsuccessful gels and failed protein expressions, even though you had no idea what I was ever talking about. I'm so excited for the next step in our lives.

Of course, I wouldn't be here without my supportive committee members. Thank you, Dr. Truman, for providing your expertise and helping me. I wish we could have actually been able to meet in person (thanks COVID). Thank you, Dr. Chi; without your wonderful cell biology class, I have no idea where I would be right now. Your enthusiasm while teaching changed my life (for the better). And last, but certainly not least, thank you Dr. Troutman for all of the support over the past two years. Thank you for always encouraging me, even after months of failed experiments and COVID issues. And thank you, especially, for not making fun of me when I 'lost' my keys

DEDICATION

For my mother, and for all the times you let me watch Jurassic Park.

TABLE OF CONTENTS

LIST OF TABLES

LIST OF FIGURES

LIST OF ABBREVIATIONS

AcCoA	Acetyl coenzyme A
Ala	alanine
BME	β-mercaptoethanol
BP	bactoprenyl phosphate
BPP	bactoprenyl diphosphate
BSA	bovine serum albumin
CDC	Center for Disease Control
CEF	cell Envelope fraction
CI	competitive index
CoASH	Coenzyme A
dNTPs	deoxy nucleotide triphosphates
DOC	deoxycholate and cholate
dTDP	deoxy thymidine diphosphate
DTNB	5,5'-Dithio-bis (3-nitrobenzoic acid)
E. coli	*Escherichia coli*
ECA	Enterobacterial Common Antigen
ECA_{CYC}	Cyclic ECA
ECA_{LPS}	ECA attached to lipopolysaccharide
ECA_{PG}	ECA attached to phosphatidyl glycerol
FT	flow-through
Glc	Glucose

Gln	glutamine
Glu	glutamate
GNATs	GCN-5-related-*N*-acetyltransferases
HILIC	hydrophilic interaction chromatography
HPLC	high-performance liquid-chromatography
IMAC	immobilized metal affinity chromatography
IPTG	isopropyl β- d-1-thiogalactopyranoside
kDa	kilodalton
LB	Luria broth
LCMS	liquid chromatography-mass spectrometry
LPS	lipopolysaccharide
MIC	minimum inhibitory concentration
NaCl	sodium chloride
Ni-NTA	nickel nitrilotriacetic acid
PBST	0.3% Tween phosphate buffer
PCR	polymerase chain reaction
PGT	phosphoglycosyl transferase
Phe	phenylalanine
PLP	pyridoxal phosphate
RCF	relative centrifugal force
RffG	a dehydratase
SDM	site directed mutagenesis
SIM	selective ion mode

TB	terrific broth
Trp	tryptophan
Tyr	tyrosine
UDP	uridine diphosphate
UppS	Undecaprenyl Pyrophosphate Synthase
WecD	an acetyltransferase
WecE	an aminotransferase
WT	wild type
WzyE	a polymerase
α-D-Fuc4NAc	4-acetamido-4,6-dideoxy-D-galactose
α-D-GlcNAc	N-acetyl-D-glucosamine
β-D-ManNAcA)	N-acetyl-D-mannosaminurinic acid

CHAPTER 1: INTRODUCTION

1.1: Bacterial Glycan Background

Bacterial glycans, the types of oligo and polysaccharides produced by both Gram negative and Gram-positive species of bacteria, are composed of rare and complex monosaccharide units, each with a unique structural arrangement. This wide variety of structures translates to a wide variety of functions. Some glycans, like colanic acid produced by *E. coli*, are excreted by the bacterium as a means of inducing biofilm formation as well as providing protection from the environment[1]. Other types of glycans can aid in establishing infection, like the capsular polysaccharide found on the surface of *Acinetobacter baumannii,* which is made of an α-branched tetrasaccharide repeat (Figure 1) [2]. The Vi Antigen, a specific glycan produced by

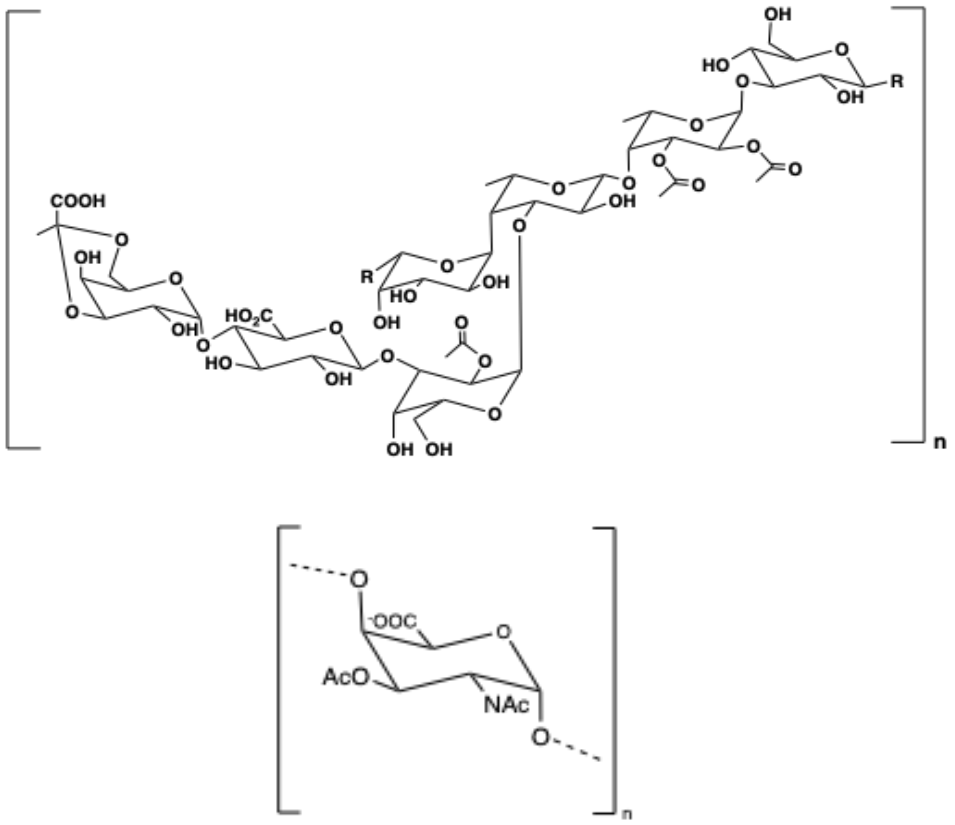

Figure 1: The tetrasaccharide subunit of the capsular polysaccharide found on *A. baumannii* (top) and the diacetylated galacturonic acid monosaccharide found on *S.* Typhi (bottom). These two structures demonstrate the wide variety of form glycans can have.

Salmonella enterica serovar Typhi, helps the bacteria evade the host immune system, and consists of multiple repeat units of a diacetylated galacturonic acid (Figure 1)[3] [4]. Due to the implications in pathogenicity and virulence, glycans can be key targets of study to help resolve a critical issue facing modern medicine: antibiotic resistance. According to the Center for Disease Control (CDC), over 35,000 people die from infections related to antibiotic resistant bacteria in the United States, alone[5]. In the European Union, there are over 25,000 deaths per year[6]. These are typically infections that should be easy to treat, and these deaths should be avoidable, if not for the emergence of resistance to common antibiotics.

Glycans can be tools of study to combat antibiotic resistance in three areas. The first being that the biosynthesis pathways of these glycans can serve as targets for novel antibiotics. While this doesn't completely solve the antibiotic resistance crisis, it can help to relieve it. This is a particularly useful tool, due to the fact that many glycans are not required for the survival of the bacteria, but may be important for infection[7]. This means that anti-virulence drugs against glycan formation would provide less selective pressure to develop resistance. The second is that glycans specific to a particular pathogen can be conjugated to proteins to become glycoconjugate vaccines. This method has already been applied with antibiotic resistant pathogens such as *Streptococcus pneumoniae* and *Neisseria meningitides*[8]. In addition to developing those types of vaccines, mutated pathogens lacking virulence-involved glycans have been tested to determine if they are acceptable candidates for live-attenuated vaccines[9]. In addition to directly fighting pathogens, the third application for bacterial glycans is less direct. This method is taking glycans, either expressed on bacteria or enzymatically synthesized and immobilized, and developing extremely specific nucleotide structures, called aptamers, against these glycans[10]. These

aptamers can be used in areas such as hospitals or water and food treatment facilities to detect the bacteria.

Most glycans follow very similar mechanisms of biosynthesis and are formed on the 55-carbon lipid anchor bactoprenyl phosphate (BP), which localizes the assembly of the glycan to the cytosolic face of the bacterial membrane (Figure 2)[11]. An initiating phosphoglycosyl transferase (PGT) will start the pathway by transferring a monosaccharide-phosphate to BP from a nucleoside diphosphate-linked sugar forming a bactoprenyl diphosphate-linked sugar. Additional glycan specific glycosyltransferases then transfer the remaining monosaccharides until a particular unit is produced. For certain glycans, the unit is polymerized, while others remain an oligosaccharide and may be transferred to proteins, lipids, or cyclized. Historically, these sugar structures have been difficult to study due to the fact that glycans are difficult to purify and separate. In the early days of glycan research, radioactively tagged isotopes of individual monosaccharides were used to track the synthesis pathway as well as which enzymes accepted which substrates[12]. Recently, the Troutman group reconstructs BP using the enzyme undecaprenyl pyrophosphate synthase (UppS), and then monitors *in vitro* reactions by liquid chromatography-mass spectrometry[11]. Another important advance in the Troutman group has

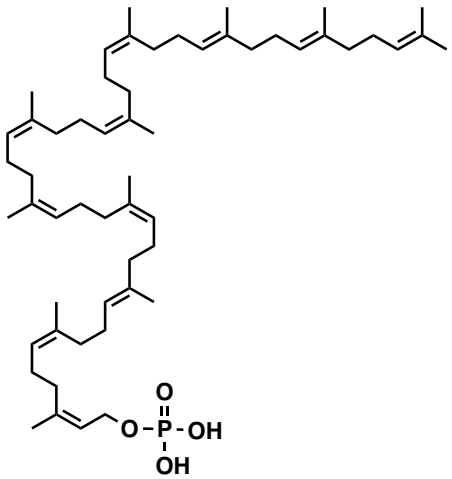

Figure 2: The 55-carbon lipid anchor bactoprenyl diphosphate

been the application of short fluorescent analogues of BP that can be monitored by high-performance liquid-chromatography (HPLC)[13]. These advances in technologies have made studying glycans, and the enzymes which make them, considerably more accessible.

1.2: The Enterobacterial Common Antigen

The Enterobacterial Common Antigen (ECA) is a glycan produced by most members of the Gram-negative bacterial family *Enterobacteriaceae* and is a polymerized trisaccharide unit containing —› 1) [N-acetyl-D-glucosamine (α-D-GlcNAc)] -4 —›1)-)- [N-acetyl-D-mannosaminurinic acid (β-D-ManNAcA)] -(4 —›1)- [4-acetamido-4,6-dideoxy-D-galactose (α-D-Fuc4NAc)-(3 —› (Figure 3) [14]. This polymerized unit can take one of three forms. It can present on the cell surface, either bound to lipopolysaccharide (LPS) (ECA_{LPS}), or to phosphatidyl glycerol (ECA_{PG})[15-16]. It can also remain in the periplasmic space in a cyclized form (ECA_{CYC})[17]. Notable members of this bacterial family which produce ECA include *Salmonella* (all serovars), *Escherichia coli* (*E. coli*), and *Klebsiella*. Although ECA was discovered in 1963, the functional role in biology of the glycan has remained poorly understood[18]. Some evidence ties it to the virulence of *Enterobacteriaceae*, more specifically, *Salmonella*[9, 14, 19]. More recently, literature has been published describing the role ECA plays in maintaining membrane permeability[20-21]. Due to the fact that ECA is found on hundreds of species of bacteria, many of which have been noted by the CDC as being serious threats in terms of antibiotic resistance, the ECA is a prime glycan to study.

Similar to other glycans, the ECA is built on a BP lipid anchor on the cytoplasmic leaflet of the bacterial inner membrane. The pathway begins with the initiating PGT WecA, which uses the nucleotide-linked monosaccharide, uridine diphosphate (UDP)-N-acetyl-glucosamine

(GlcNAc), to attach GlcNAc -phosphate to BP (Figure 4). This interaction forms BPP-GlcNAc (ECA Lipid I). The next sugar to be added, ManNAcA, is formed by the epimerase WecB and dehydrogenase WecC. WecB catalyzes conversion of UDP-GlcNAc to UDP-N-acetyl-mannosamine (ManNAc) and WecC catalyzes the conversion of UDP-ManNAc to UDP-N-acetyl-mannosaminouronic acid (ManNAcA). The glycosyltransferase WecG then catalyzes the transfer of ManNAcA to the 4' position of the GlcNAc in ECA Lipid I to form ECA Lipid II.

The final sugar appended to the repeat unit of ECA forming ECA Lipid III is a 4-N-acetyl-fucosamine, which is transferred by the glycosyltransferase WecF. Fuc4NAc is a rare bacterial sugar produced by three enzymes from the starting nucleotide-linked sugar deoxythimidine diphosphate (dTDP)-Glucose (Glc). dTDP-Glc is converted to dTDP-keto-6-deoxy-Glc by the dehydratase RffG. This keto product is then aminated by the aminotransferase WecE to form dTDP-Fuc4NH_2. The final step in dTDP-Fuc4NAc assembly is then catalyzed by the acetyltransferase WecD which transfers an acetyl group from AcCoA to the aminated sugar.

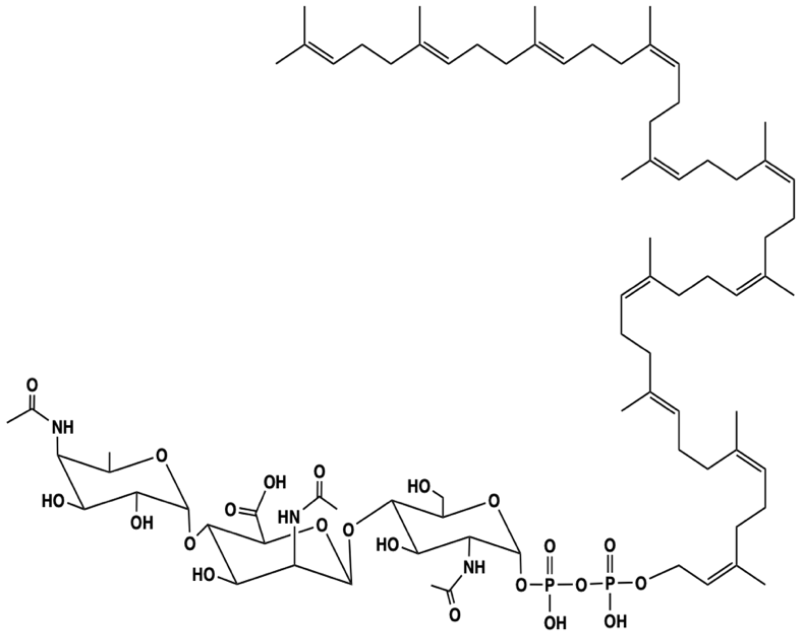

Figure 3: The ECA trisaccharide unit (α-D-GlcNAc -(4 —›1)- β-D-ManNAcA- (4—›1)-α-D-Fuc4NAc) covalently attached to BPP

Once the repeating unit of ECA is formed by WecF, ECA Lipid III is flipped into the periplasmic space by the flippase WzxE and is polymerized by the polymerase WzyE. The length of the polymer is regulated by the co-polymerase WzzE, before the pathway splits to produce one of the three forms of the ECA[16]. The oligosaccharide can be attached to lipopolysaccharide (LPS) via the enzyme WaaL and then be presented on the cell surface as ECA_{LPS}[15]. This form of the ECA is the only one that has been demonstrated to illicit an immunogenic response in animal studies[15, 22-23]. The ECA can also be present on the cell surface while covalently attached to phosphatidyl glycerol as ECA_{PG}, however the mechanism for attachment is unknown. Alternatively, the ECA could remain in the periplasmic space in a cyclized form (ECA_{CYC}), which is a poorly understood process involving WzzE [17, 20].

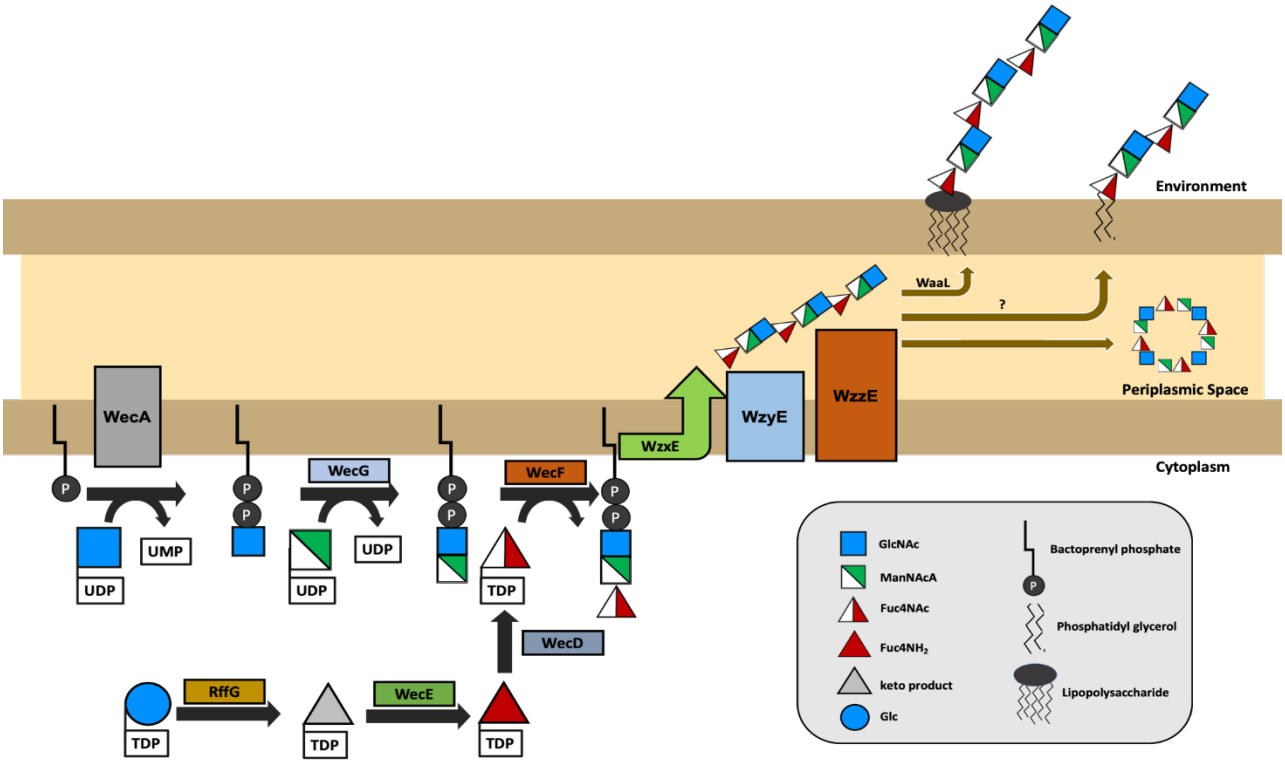

Figure 4: The ECA biosynthesis pathway

There have been numerous studies that demonstrate that individual deletions of genes required for ECA production result in important biological consequences. It was found in 1998 that the deletion of the *E. coli* genes *wecF*, *wecE*, or *rmlA* (encodes the protein responsible for formation of dTDP-Glc) triggers the stress response pathways Cpx and σ^E. These pathways are responsible for increasing the levels of the heat shock periplasmic protein DegP by upregulating the transcription of the inducible gene *degP*[24]. This results in the *E. coli* having a higher sensitivity to bile salts. However, it was unclear of whether these results were due to the lack of the ECA, or the accumulation of ECA Lipid II.

More recently, studies have demonstrated that the biological consequences of ECA biosynthesis gene deletions are often the result of the accumulation of intermediate lipids like ECA Lipid II, as this results in the sequestration of the lipid anchor BP from other cellular pathways, particularly from peptidoglycan synthesis[7]. Even though many biosynthesis pathways in bacteria require BP, once a particular biomolecule is formed BP is recycled and used for other pathways. Therefore, if a pathway is disrupted through deletion of genes that halt the pathway, BP is unable to be recycled and redistributed, and the bacteria would be affected. More evidence for this was provided in 2016 by the Young group, when researchers studied the morphological effects that single deletions of *wec* genes in *E. coli* have. They found that when the gene *wecE* was deleted (which is required for Lipid II synthesis), the bacteria were unable to divide normally, resulting in morphological defects. However, a double *wecAwecE* mutant did not have this defect. This suggests that the lack of available BP for other cellular processes, specifically the production of peptidoglycan, has major biological implications[7]. More recently, the Troutman lab has found that each subsequent dead-end ECA mutant (*wecA, wecG, wecF, wzxE*) results in lower and lower levels of cellular BP[25].

In addition to the sequestration of BP, additional evidence suggests that changes in membrane permeability can be attributed to ECA_{CYC} and the enzyme YhdP[20]. In 2018, it was found that the gene *yhdP* co-occurs with the *wec* operon and can influence the levels of ECA in bacteria. When *wzzE* is absent in bacteria, they are no longer able to adjust the permeability of the outer membrane. ECA_{CYC} is the sole product of WzzE, and therefore the researchers concluded that ECA_{CYC} plays a role in regulating the permeability of the cell. The authors postulated that ECA_{CYC} may act in a similar manner to cyclodextrins and can pull membrane - disrupting molecules from the membrane for disposal. This literature was the first to provide evidence for a direct biological role of ECA. In addition to the role ECA plays in membrane permeability (whether due to the build-up of ECA intermediate lipids or the lack of ECA_{CYC}), ECA has also been shown to be connected to the virulence of *Salmonella enterica*. First published in 1976, it was found that *Salmonella* lacking ECA were unable to infect mice through oral infections. In 2003, these results were corroborated, and then again in 2020[14, 19].

1.4: dTDP-Fucosamine Acetyltransferase and Its Role in ECA Production

The dTDP-Fucosamine Acetyltransferase, WecD, is responsible for catalyzing the conversion of dTDP-Fuc4NH_2 to dTDP-Fuc4NAc, which is the final sugar added to the ECA trisaccharide repeating unit[26]. It was first discovered that the gene *wecD* (previously *rffC*) encoded the conversion of dTDP-Fuc4NH_2 to dTDP-Fuc4NAc in 1989[12]. Although there have been many studies involving WecD *in vivo*, it has never been characterized *in vitro*. However, *in vitro* work is warranted due to the connection between *wecD* and *Salmonella enterica* virulence. In previous studies, any detrimental effects of an ECA gene deletion in *E. coli* can be reversed by an accompanying deletion of the gene *wecA*. Without *wecA*, the ECA pathway cannot begin, and

therefore there is no accumulation of intermediate lipids. However, a study in 2003 described a new phenotype associated with *wecD* deletion when screening for bile salt resistance genes in *Salmonella*. They found that when *wecD* is deleted, the minimum inhibitory concentration (MIC) of deoxycholate and cholate (DOC) was 0.1% DOC. This significantly differed from that of the wild-type (WT) *Salmonella* which could withstand up to 4% DOC. If the bile resistance was due to ECA Lipid II accumulation, then deletion of *wecA* would not alter DOC resistance relative to WT. However, when *wecA* was deleted *Salmonella* could only withstand 0.2% DOC. These results suggested that in *Salmonella*, the sensitivity to DOC was due to the lack of the ECA, and not the accumulation of an intermediate lipid.

Since DOC resistance was used as a model for bile acids it was important to determine whether disruptions in ECA affected the ability of *Salmonella* to infect animals. Mice were infected both orally and intraperitoneally with ECA deletion strains and WT strains to determine the competitive index (CI) of each mutant. These values are sensitive measurements of virulence, which are determined by using the ratio of mutant to WT bacteria post-infection and dividing it by the ratio at the beginning of the infection. It was found that both the *wecD* and *wecA* mutant strains were significantly more attenuated than the WT strains of *Salmonella* (P-value of a Student's T-Test both <0.05). When the *wecD* and *wecA* strains were directly compared to one another, the CI of the *wecD* strain was similar to the CI of the *wecA* strain (P-value = 0.09). These results provided evidence that ECA is an important virulence factor in *Salmonella enterica,* and attenuation was not due to accumulation of Lipid II. For these reasons, we believe that the enzyme WecD could be a viable target for a small-molecule inhibitor to have an anti-virulence mechanism. By inhibiting the enzyme WecD, the ECA pathway is halted at ECA Lipid II, therefore causing *Enterobacteriaceae* species to be susceptible to the environment, as well as

potentially mimicking the attenuation results found in the *Salmonella*. Therefore, this work will partially focus on the expression and characterization of WecD. This will allow for accurate screening of inhibitors, and potentially may allow for design of WecD-specific inhibitors.

1.5: Characteristics of WecD

WecD belongs to a large enzymatic family of GCN-5-related-*N*-acetyltransferases (GNATs). GNATs are found in every kingdom of life, and all share the common task of acetylating a primary amine. Common GNATs include histone acetylases and serotonin acetyltransferases[27-28]. WecD sequence identity is approximately 40% or greater across *Enterobacteriaceae*[26]. In 2006, the crystal structure of uropathogenic *E. coli* WecD was determined, as well as the most-likely binding patterns of both WecD substrates, acetyl coenzyme A (AcCoA) and dTDP-FucNH_2. The crystal data revealed that WecD exists as a

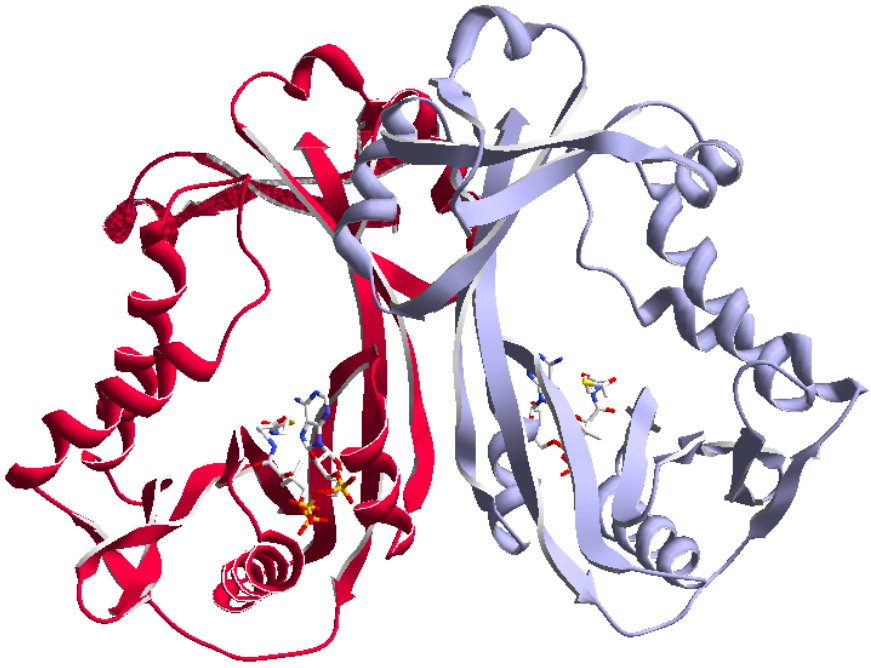

Figure 5: The WecD ribbon structure displaying each chain of the dimer (red and purple). AcCoA can be seen entering one side of each monomer of WecD.

homodimer in solution and is an α/β class. A single monomer consists of 5 β sheets and 4 α helices. The two monomers connect via interactions between β4 and β10, and also α3 and α7. For catalysis to take place, both dTDP-Fuc4NH$_2$ and AcCoA must enter WecD at opposite ends of a catalytic tunnel and meet in the middle. AcCoA will interact with residues found on β8, β9, and α4-7, which are found near the C-terminus of WecD (Figure 5), AcCoA will take a bent conformation at the P2 or the diphosphate moiety as it forms hydrogen bonds with the backbone atoms on β8 and α6 residues, which is unique to WecD and not found with other GNATs. A key residue in AcCoA stabilization is Tyr208, which is suggested to form a hydrogen bond with the sulfur atom of AcCoA. This is thought to be a significant interaction in stabilizing the reaction between dTDP-Fuc4NH$_2$ and AcCoA[26]. Based on computer simulations, dTDP-Fuc4NH$_2$ is thought to enter the catalytic tunnel in a chair conformation and forms hydrogen bonds with Ala196, Glu70, Tyr123, and Phe104. The thymine moiety is thought to form parallel stacks with the residues Phe122 and Trp2126, which may provide a key stabilizing factor for the WecD reaction. Alternative parallel stacking could occur between the thymine moiety and Trp126 and Phe135, instead. When the two substrates meet in the center of the tunnel, the primary amine of

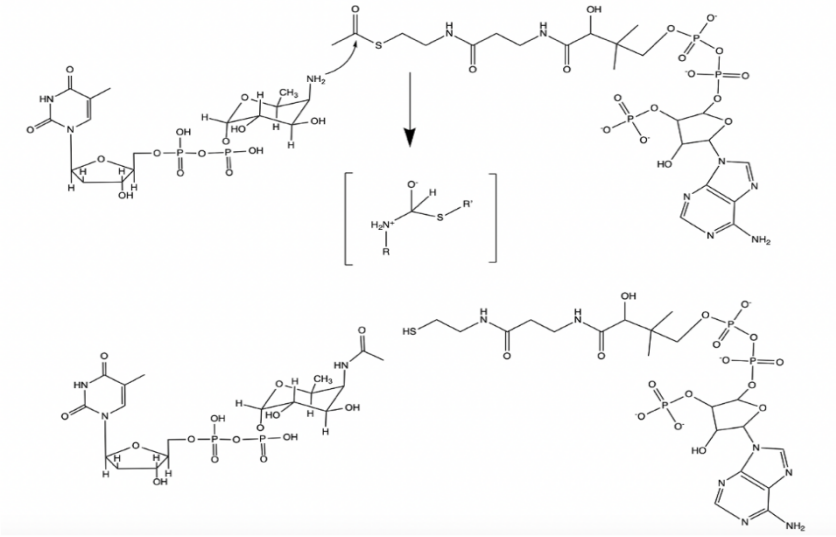

Figure 6: Catalytic mechanism of WecD. Deprotonated NH2 acts as a nucleophile on the thioester of AcCoA. The 2 substrates form a tetrahedral intermediate, before dTDP-Fuc4NAc and CoASH leave.

dTDP-Fuc4NH_2 is deprotonated to act as a nucleophile attacking the thioester of AcCoA (Figure 6). In order for this to occur, the ammonium group must be deprotonated by a nearby acidic residue, which is most likely Glu68. After the tetrahedral intermediate is formed, the thiolate leaving anion is thought to be stabilized by Tyr208, and Coenzyme A (CoASH) and dTDP-Fuc4NAc leave the tunnel.

1.6: The ECA Polymerase: WzyE

The final step in ECA assembly is polymerization by the enzyme WzyE. After the BPP-linked trisaccharide unit is flipped into the periplasmic space by the flippase WzxE, WzyE polymerizes ECA Lipid III so that it can be further modified by other enzymes to form $ECA_{LPS,}$ ECA_{PG}, and ECA_{CYC}. The ECA, like many other glycans, follows a Wzx/Wzy-dependent polymerization pathway. The Wzx flippase is proposed to recognize the first sugar of the repeat unit to initiate the process[29]. Despite multiple *in vivo* studies confirming the role Wzy-type polymerases play in glycan synthesis, there have been only a few *in vitro* studies[30]. This is due, in part, to the fact that these proteins can have over 10 transmembrane domains. WzyE, in particular, has 13 predicted transmembrane domains (Figure 7) [29]. The difficulty with proteins with multiple transmembrane domains is that they can be impossible to purify in a functional form away from the membrane itself as the membrane aids with maintaining the structure. One study, which successfully expressed another Wzy-type polymerase, truncated the protein and used co-expressing chaperone proteins to promote appropriate folding to study it *in vitro*[30].

In addition to Wzy-type polymerases being difficult to express *in vitro*, the substrates for these enzymes have been historically difficult to obtain. Only very recently has the Troutman laboratory accomplished enzymatically synthesizing the ECA trisaccharide *in vitro*[25]. These

glycans can, hypothetically, be chemically synthesized without the aid of enzymes, but this is not a practical process and is costly and time intensive, with many synthetic manipulations involved[31].

Aside from being the next step in studying the ECA *in vitro*, obtaining a functional WzyE to form a polymerized ECA provides another valuable tool: the ability to produce large quantities of pure ECA at a given time. Synthetically making the ECA is impractical, but so is isolating the ECA from bacteria. The three types of the ECA have very different characteristics and are difficult to purify. Additionally, it is difficult to determine whether or not there is a pure sample of just ECA, as other glycans could be in the sample as well. Henceforth, using the WzyE *in vitro* not only allows for the potential to make the ECA in larger quantities, but could lead to more studies on Wzy-type polymerases to make other glycans in larger quantities.

CHAPTER 2: MATERIALS AND METHODS

2.1: *wecD* and *wzyE* Plasmid Transformations

pET15b vector plasmids were purchased from Gene Universal Inc. Ten ng of each plasmid was then transformed into 40 µL of chemically competent DH5α and C41 *E. coli* cells. *wzyE* was also transformed into competent Δ*wecA* strain of C41 *E. coli*. The transformation was plated on agar-plates containing 50 µg/mL carbenicillin and grown at 37°C overnight. A colony from each transformation was then added to 2 mL Luria-Broth (LB) containing carbenicillin, which grew for 8 hours. 1 mL of each culture was used to make a glycerol stock and stored at -80°C.

2.2: Expression and Preparation of Enzymes

2.2.1: WecE, RffG, and WecD Expression

5 mL cultures of Luria Browth (LB) containing 50 µg/mL of antibiotic (kanamycin for WecE and RffG; carbenicillin for WecD) were inoculated using C41 *E. coli* glycerol stocks and grown at 37°C while shaking overnight. The next morning, the cultures were diluted 1:100 in LB and the respective antibiotic. The cultures were grown to an OD_{600} between 0.4 and 0.6 before being induced with 1mM isopropyl β- d-1-thiogalactopyranoside (IPTG) and were cultured for 16 hours at 16 °C. The cultures were then spun at 5000 relative centrifugal force (RCF) for 15 minutes at 4 °C; the pellets were resuspended in lysis buffer (50 mM Tris, pH 8, 20 mM imidazole, 200 mM sodium chloride). After being sonicated at 25% amplitude for 3 minutes, the proteins were spun at 91,635 RCF for 60 minutes at 4 °C.

After centrifugation, the supernatant was poured over a nickel nitrilotriacetic acid (Ni-NTA) column, the cell pellet was discarded, and the flow-through (FT) was collected in a plastic beaker. A wash buffer (50 mM Tris, 50 mM imidazole, 200 mM NaCl) was poured over the

column and was collected. Six elutions were collected in microcentrifuge tubes using an elution buffer (50 mM Tris, 500 mM imidazole, 200 mM NaCl). The FT, W, and six elutions were then analyzed via SDS-PAGE to determine which fraction contained the isolated protein. Dialysis was then performed on the appropriate sample to remove imidazole. The dialysis buffer for RffG consisted of 50 mM Tris pH 8 and 300 mM NaCl; dialysis buffer for WecE and WecD consisted of 50 mM Bicine pH 9 and 200 mM NaCl. The concentrations of the proteins were determined using a Nano Drop spectrophotometer at 280 nm.

2.2.2: WzyE Expression

A 5 mL starter culture containing terrific broth (TB) (24 g/L yeast extract, 20 g/L tryptone, 4 mL/L glycerol, 90 mM phosphate buffer) and 100 μg/mL carbenicillin was inoculated with C41 *E. coli* containing the *wzyE* pET15b plasmid and cultured overnight at 37 °C while shaking. The following morning, the starter culture was diluted 1:1000 in 500 mL TB with 2% glucose to prevent premature plasmid expression and was incubated at 37 °C while shaking, until an OD_{600} of 1 was reached. The culture was then induced using 1 mM IPTG, and the culture was incubated at 16 °C overnight, while shaking. After growing overnight, a 1 mL post-induction sample was taken. The culture was spun at 5,000 RCF for 15 minutes at 4°C.

To check for induction of expression, 5 50 mL cultures of *E. coli* containing the wzyE-pET15b plasmid were inoculated as described previously. One culture contained 1% glucose, the other three were just TB. The 4 cultures were cultured as described above, with a 1 mL sample taken before induction with IPTG, and a 1 mL sample taken after 16 hours. A 50 μL 50/50 dilution of the pre- and post-induction samples with lysis buffer was prepared, and then placed in a water bath sonicator for 10 minutes. 75 μL of 1X SDS-PAGE buffer was added to the pre-

induction sample, while 586 μL of 1X SDS-PAGE buffer was added to the post induction sample. The samples were then placed on a heat block at 90 °C for 15 minutes and then spun at 5000 RCF for 5 minutes. The samples were then analyzed using SDS-PAGE to confirm induction.

The remaining cell culture was pelleted, resuspended, and lysed as described above before being spun at 2500 RCF for 10 minutes to remove large cell debris. The supernatant was then transferred to an ultracentrifuge tube and spun at 91,635 RCF for 60 minutes at 4 °C. The cell pellet was then homogenized in 2 mL dialysis buffer (50 mM Tris, 300 mM NaCl) to form the cell envelope fractions (CEF) and stored at -80 °C.

Table 1: Strains of bacteria used in this work

Strain Number	*E. coli* strain	Plasmid	Gene Insertion	Genotype	Antibiotic Resistance
JT337	DH5α	pET15b	*wecD*		Carbenicillin
JT339	DH5α	pET15b	*wzyE*	Δ*wecA*	Carbenicillin
JT338	C41	pET15b	*wecD*		Carbenicillin
JT341	C41	pET15b	*wzyE*	Δ*wecA*	Carbenicillin
JT263	C41	pET24a	*rffG*		Kanamycin
JT261	C41	pET24a	*wecE*		Kanamycin
JT271	MG1655	pMAJ9	$uppS_{EC}$	MG1655 ΔWzxe::frt:: pMAJ9 (Kan^R)	Carbenicillin

Table 2: Protein expression conditions

Protein	Strain	6His-Tag	Media	IPTG	Hours	Temperature (°C)
WT WecD	JT338	N-term	LB	1 mM	16	16
WecE	JT261	C-term	LB	1 mM	16	16
RffG	JT263	C-term	LB	1 mM	16	16
WzyE	JT341	N-term	TB	1 mM	16	16

2.2.3: SDS-PAGE and Western Blot of Enzymes

After protein purification, 10 μg of each protein was analyzed using SDS-PAGE. The proteins were also transferred to a nitrocellulose for a Western blot; a Ponceau stain confirmed transfer. The nitrocellulose membrane was blocked by rocking in 5% milk dissolved in 0.3% Tween phosphate buffer (PBST) overnight at 4 °C. The membrane was incubated in a 1:5000 dilution of primary mouse anti-His tag antibody for 24 hours at 4 °C, and then in a 1:20,000 dilution of secondary goat anti-mouse antibody conjugated to alkaline phosphatase for six hours. The Western Blot was developed in NBT/BCIP until color appeared corresponding to the presence of the tagged protein.

2.2.4: WecD His-Tag Cleavage

A Sigma-Aldrich Thrombin CleanCleave kit was used to remove the 6His tag from WecD. 100 μL of a 50/50 thrombin-agarose suspension was incubated with 1 mg of WecD protein and 100 mM $CaCl_2$ at 37 °C while rocking. The reaction was spun at 2500 RCF for 30 seconds to pellet the thrombin-agarose, and the supernatant was removed and passed over a Ni-NTA column to remove any uncleaved protein. The flow-through was dialyzed using the same

dialysis buffer described above. SDS-PAGE and a Western Blot (as described above) were used to confirm His-tag cleavage.

2.3: Enzymatic Reactions

2.3.1: Synthesis of dTDP-Fuc4NH_2 and UDP-Fuc4NH_2

The enzymatic reactions to synthesize dTDP-Fuc4NH_2 used 1 mM dTDP-Glc, 100 mM glycine pH 10, 10 mM $MgCl_2$, 14 mM glutamate, 500 μM PLP (pyridoxal phosphate),1 μM RffG, and 1 μM WecE. An aliquot of the reaction without enzyme was set aside as a control. The RffG was added first and incubated at 37 °C for 30 minutes. An aliquot of the RffG reaction was set aside, and WecE was added to incubate at 37°C for another 30 minutes. After each reaction was complete, it was diluted 1:4 in 125 mM ammonium acetate pH 4.5. Each reaction was analyzed using an Agilent 1100 series high-performance liquid-chromatography (HPLC) system and an Agilent Zorbax NH_2 column (4.6 x 150 mm, 5 μm). The mobile phase was 250 mM ammonium acetate pH 4.5 and was used at a flow of 1 mL/minute. Absorbance of the eluting products was measured at 260 nm. Pure dTDP-Glc was used as a standard. The dTDP-Fuc4NH_2 product was isolated in real time and lyophilized to remove mobile phase and the majority of salts. The RffG, WecE, and WecD reactions were also injected onto an Agilent 1260 Infinity II liquid chromatography-mass spectrometry (LCMS) system using an Agilent Poroshell 120 HILIC-Z column (4.6 x 50 mm, 2.7 μm) and selective ion mode (SIM) to confirm the product with mass. A similar process was used to use UDP-Glc to turnover UDP-Fuc4NH_2, however this was accomplished using 3 mM UDP-Fuc4NH_2, 28 mM glutamate 1 mM PLP, and 20 μM of RffG and WecE. UDP-Fuc4NH_2 was purified as described above, and then injected directly onto the mass spectrometer of the LCMS to confirm the product.

2.3.3: WecD Enzymatic Reactions

The typical WecD enzymatic reactions were performed as follows: Fuc4NH_2 (dTDP or UDP), acetyl coenzyme A (AcCoA) (10 μM – 160 μM), 100 mM Tris pH 6.8, and WecD (1 μg) (Table 3). The reaction proceeded at 37°C for 30 minutes and was then quenched in 125 mM ammonium acetate pH 4.5 as described above and checked using HPLC. An aliquot of the reaction without enzyme quenched in 125 mM ammonium acetate pH 4.5 was used as a control.

Table 3: WecD reaction conditions

[WecD]	[X-Fuc4NH_2]μM	[AcCoA] (μM)	pH	WecD Construct
0.1 μg	UDP, 10	20	6.8	Cleaved pET24a uncleaved pET15b uncleaved
	dTDP, 10, 20*	10		
		20		
		40		
		80		
		160		

2.3.4: WecD Kinetic Assays

Two kinetic assays were developed to study WecD. In one well of a 96-well plate, a WecD reaction lacking AcCoA was prepared to have a final volume of 65 μL was prepared and contained 0.5 mM 5,5'-Dithio-bis (3-nitrobenzoic acid) (DTNB, Ellman's Reagent, Sigma-Aldrich). In an adjacent cell, 15 μL of AcCoA was added. After incubating at 37° C for 5 minutes, 13 μL AcCoA was added to the WecD well to initiate the reaction. The control reaction consisted of a reaction lacking WecD. The absorbance was monitored on a Molecular Devices SpectraMax M5 plate reader at 412 nm every 10 seconds for 10 minutes. The reaction was then quenched using ammonium acetate and checked on HPLC. Concentration of product was calculated via linear regression from quantified standards of β-mercaptoethanol (BME)[27].

The other assay was a discontinuous assay that used the HPLC, as described above. A 30 μL WecD reaction was set up lacking WecD in a microcentrifuge tube. In a different tube, WecD and amount of water needed to bring the volume to 30 μL was added. Both tubes sat in a heat block at 37 °C for 5 minutes. WecD was then added to the rest of the reaction. At the 30 min, 60 min, and 120 min time points, 7 μL of the reaction was removed and quenched in 10 μL ammonium acetate pH 4.5. The reaction was then analyzed in the HPLC, where the areas under the Fuc4NH_2 and Fuc4NAc curve were measured and used to calculate the percentage of product turnover.

2.3.5: Polymerization of Native Lipid III

Native Lipid III was prepared by inoculating a 5 mL culture of LB and 100 mM MOPS buffer with Δ*wzxE* strain of *E. coli* transformed with a PMAJ9 plasmid with a UppS insertion to prevent the morphological defects typically found in ECA-enzyme deficient strains. To maintain

the presence of the plasmid and induce *uppS* expression, 50 μg/mL carbenicillin and 1 mM IPTG were included. After growing overnight at 37 °C with shaking, the bacteria were pelleted at 5000 RCF for 15 minutes and washed with PBS. The cells were then resuspended in a 2:1:1 ratio of chloroform, methanol, and water, and left at room temperature for 20 minutes. The aqueous phase was removed with a glass pipette, dried under a vacuum, and resuspended in 1 mL 25% propanol with 1% ammonium hydroxide. 50 μL of the solution was then analyzed using an Agilent 1260 Infinity II LCMS using a Waters Xbridge BEH C18 column (4.6 mm x 50 mm, 3.5 μm, 300 Å). The mobile phase consisted of 85% 100 mM ammonium hydroxide and 15% *n*-propanol; over 20 minutes the *n*-propanol concentration increased from 15% to 95%. To perform the WzyE reaction, 20 μL of the Native Lipid III was placed in a microcentrifuge tube and dried under air. The Lipid III was resuspended in 20 mM Tris HCl pH 7.5, 100 mM NaCl, and 10 mM $MnCl_2$. The reaction was then split into two tubes. In one, enough water to bring the final volume to 50 μL was added, the other with 25% propanol to quench the reaction to act as a control. Then, 20 μL of WzyE CEF was added to each tube. The reaction progressed at 37 °C for 1 hour, with aliquots being removed at 0 min, 30 min, and 60 min. The reaction was monitored by LCMS as described above to detect any differences in free BP, BPP, and Lipid III in solution.

Table 4: Ions monitored on the LCMS

Molecule	Ion(s) monitored
BPP	925.6
BP	845.7
ECA III	1532.8

2.4 Statistical Analysis

The statistical software program SPSS Statistics was used for the statistical analyses. The turnover at WecD reaction time points were compared to one another using either independent t-tests (dTDP-Fuc4NH_2 vs UDP-Fuc4NH_2) or an ANOVA test (the different WecD constructs).

CHAPTER 3: RESULTS AND DISCUSSION

3.1: Preparation of ECA synthesis proteins

The focus of this thesis is on the analysis of the proteins WecD and WzyE, key proteins in the assembly of the ECA polymer. In order to focus on these proteins, the ability to isolate each and its substrates was required. To prepare substrates, previous researchers in the Troutman group prepared *E. coli* strains capable of overexpressing all ECA genes, except WzyE, using a pET-24a vector which encodes a C-terminal hexahistidine tag used for purification by immobilized metal affinity chromatography (IMAC) (Figure 7). Previous researchers have also shown that the isolated enzymes were active and could be used to effectively prepare substrates for WecD and WzyE. However, early investigations into WecD activity, as will be described later in this thesis, suggested that the purification tag on WecD was problematic for rapid methods to analyze its function.

Figure 7: The pET15b (TOP) and pET24a (BOTTOM) constructs of WecD not drawn to scale

Due to problems with the initial WecD, a new construct was prepared that would allow for removal of the purification tag after protein isolation. This same system was used for the production of WzyE. Genes encoding WecD and WzyE were commercially synthesized and inserted into a pET-15b vector (Figures 7). The pET-15b vector harbored a carbenicillin resistance gene as a selectable marker and provided for a thrombin cleavable N-terminal hexahistidine tag. Plasmids containing *wecD* and *wzyE* were transformed into DH5α *E. coli* strains to provide a renewable stock of the plasmids, and C41 B-strain *E. coli* for protein expression. The C41 strain has been especially amenable to these types of proteins in our laboratory previously. In addition, we also transformed the *wzyE* plasmid into a C41 *E. coli* strain with the *wecA* gene deleted from the genome. This strain was utilized for the expression WzyE to avoid complicating factors associated with endogenous ECA expression when isolating the protein and analyzing its function. To select for positive transformants the cells were plated on LB Agar plates containing carbenicillin and were incubated overnight. Colonies that grew on the selective media were presumed to contain the plasmid based on the selectable marker and were collected. Control transformations (no plasmid transformed) were also prepared and resulted in no colony growth.

To prepare for the analysis of WecD and WzyE each protein along with the enzymes RffG and WecE (required to make the WecD substrate dTDP-Fuc4NH_2) were expressed in C41 B-strain *E. coli* cells. With the exception of WzyE, all ECA synthesis proteins had been successfully expressed and purified in the Troutman laboratory previously. Using standard culture and induction protocols each gene was overexpressed and purified by IMAC (Ni-NTA), except WzyE which was prepared as a membrane fraction and not further purified. Analysis of

the isolated RffG, WecE, and WecD (uncleaved) by SDS-PAGE and Anti-His Western Blot indicated the production of a protein with the expected molecular weight (Figure 10, Table 5).

The expression of WecD yielded 2.5 mg/mL of pure protein. To cleave the purification tag, the WecD preparation was treated with magnetic bead-conjugated thrombin protease and analyzed by SDS-PAGE. To obtain pure, untagged WecD the incomplete reaction was passed over a nickel column to separate the His-tagged protein from the cleaved protein. Due to the lack of the 6-His tag, the cleaved WecD eluted in the flow-though (Figure 8). After dialysis, 1 mg of uncleaved protein yielded 0.15 mg of cleaved WecD. The 6-His tag weighs approximately 0.8 kDa, therefore when the cleaved and uncleaved proteins are compared using SDS-PAGE, there is a slight size difference, reflecting the cleavage of the tag (Figure 8).

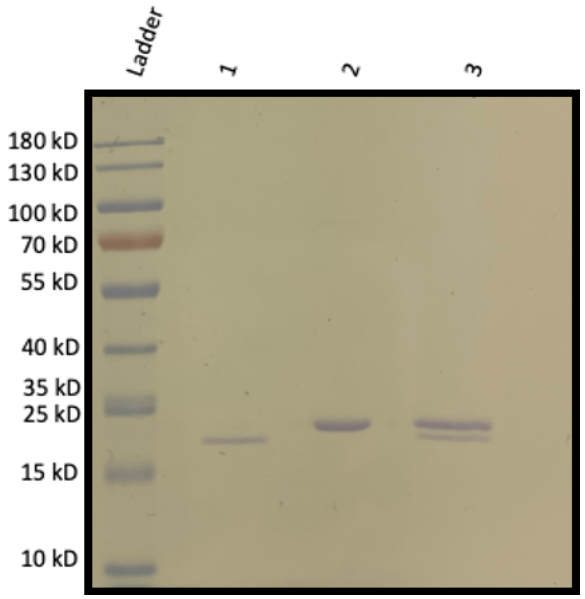

Figure 8. SDS-PAGE of the WecD protein before and after the thrombin cleavage reaction. LANE 1: Cleaved WecD. LANE 2: Uncleaved WecD. LANE 3: 1:1 mix of the cleaved and uncleaved WecD.

WzyE was expected to be fully embedded in the *E. coli* cell membrane. To test for its overexpression, we analyzed its production through pre- and post- induction analysis (Figure 9). We noted two bands that appeared post-induction and it was unclear which of these bands was WzyE. The upper band, around 50 kDa, was close to the expected molecular weight of WzyE (51.9 kD), while the lower band was closer to 37 kDa. However, membrane-bound proteins have been shown to be less affected by the denaturing of SDS and are therefore more compact. This

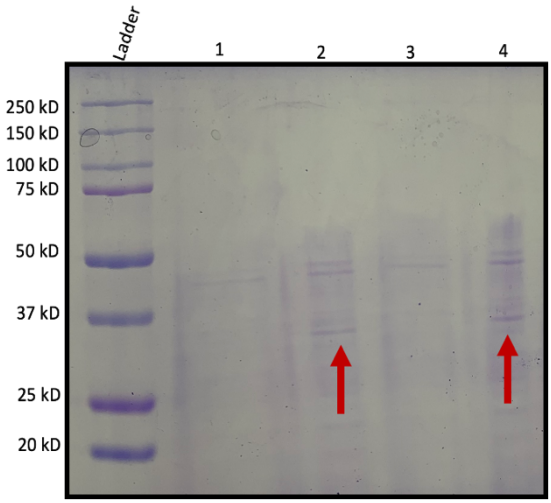

Figure 9: Pre- and post-induction samples of WzyE Expression. 1: Pre-induction sample of culture containing 2% glucose. 2: Post-induction sample of culture containing 2% glucose. 3: Pre-induction cultures without glucose. 4: Post-induction cultures without glucose.

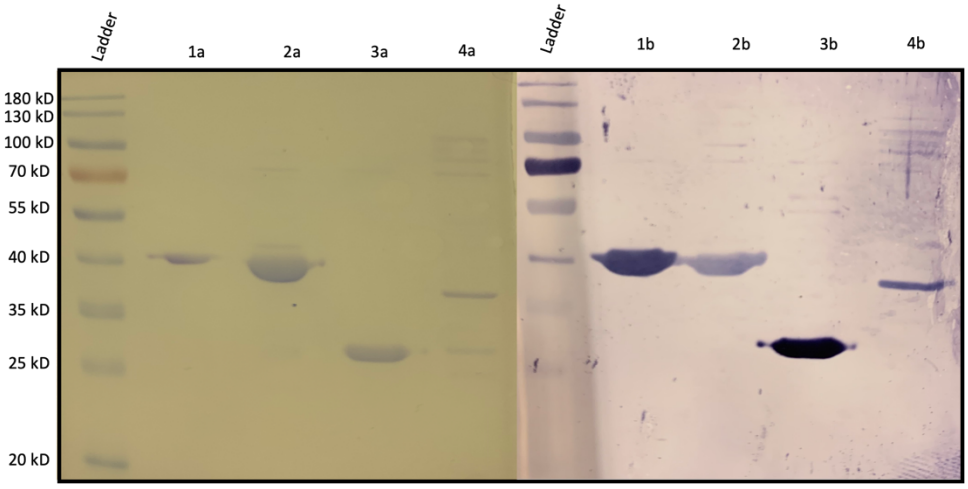

Figure 10: LEFT: SDS-PAGE analysis of RffG (1a), WecE (2a), WecD (3a), and WzyE MF (4a). RIGHT: Western Blot of RffG (1b), WecE (2b), WecD (3b), and WzyE MF (4b

can allow for the proteins to travel more quickly through the acrylamide gel, giving the appearance of having a lower molecular weight[32]. An anti-His western blot confirmed that the lower band correlated with WzyE (Figure 10). However, because the protein has an N-terminal hexahistidine tag it was not possible to rule out protein truncation.

Table 5: All the ECA enzymes used. Column 1: Name of the proteins. Column 2: Molecular weight of the proteins (kDa). Column 3: Soluble or membrane fraction protein. Column 4: Concentration after expression (μM)
*WecD concentration pre-cleavage
**WecD concentration post-cleavage

Enzyme	Size (kDa)	Type of Protein	Culture Volume	Concentration
RffG	39.7	Soluble	1 L	325 μM
WecE	41.9	Soluble	1 L	180 μM
WecD	24.2	Soluble	1 L*, 1 mL**	60 μM *, 2.25 μM **
WzyE	51.9	Membrane	500 mL	13 μg/μL

3.2: Enzymatic Reactions

3.2.1: WecD Substrate Preparation

The substrate for WecD, dTDP-Fuc4NH_2, is not commercially available and therefore needed to be prepared in our laboratory. dTDP-Glc is commercially available and could be converted to dTDP-Fuc4NH_2 through the activity of the enzymes RffG and WecE (Figure 11). To analyze these reactions, we used a method previously described by our group for the analysis of similar enzymes[25]. This method utilizes HPLC with a propylamine-based column (NH2-HPLC) which can separate closely related nucleotide-linked sugars. To test our RffG and WecE, a reaction mixture was prepared with each protein and the substrate dTDP-Glc. After 30 minutes

of incubation at 37 °C, an aliquot of the mixture was analyzed by NH2-HPLC and product was detected by the change in retention time of the thymidine ring observed at 260 nm (Figure 12). A control reaction, which lacked any enzyme, resulted in a dTDP-Glc peak eluting at 19.9 minutes. With the addition of RffG, the product had a slight increase in retention time to 20.0 min. Due to the small structural differences in dTDP-Glc and the RffG product (a hydroxyl group versus a ketone, respectively) a small shift in retention time is to be expected, and this small shift was consistent with previous experience of our group with similar enzymes[25].

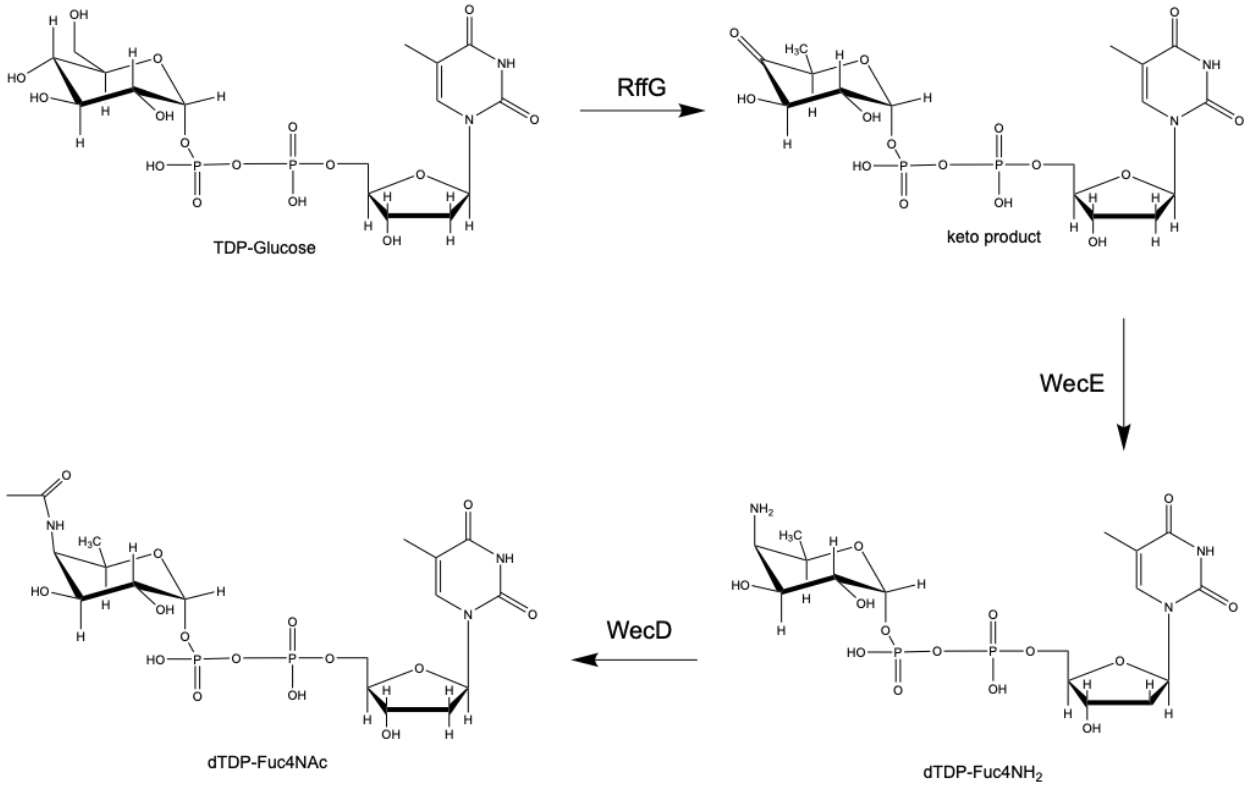

Figure 11: dTDP-Fuc4NAc synthesis pathway

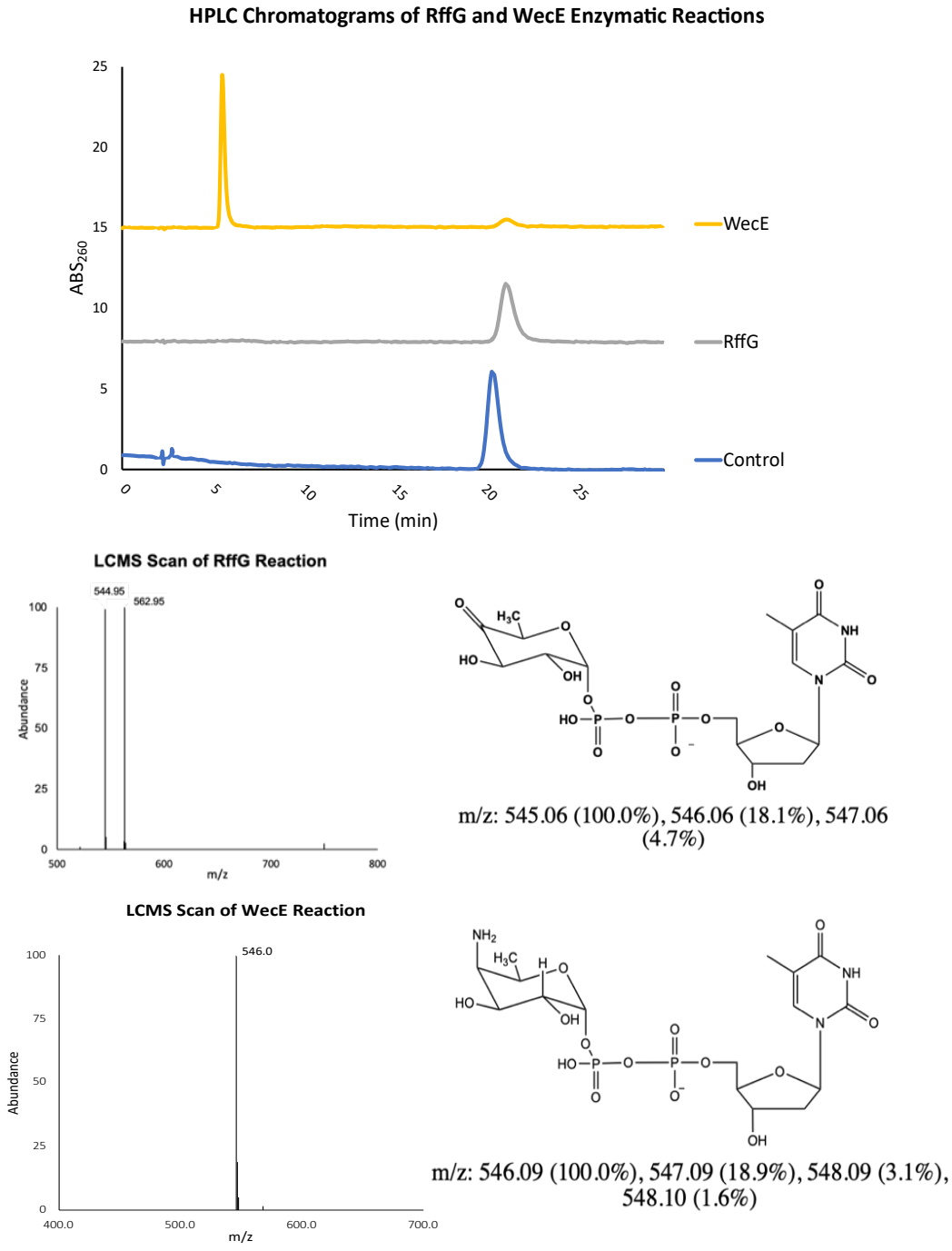

Figure 12: TOP: HPLC Chromatograms of the RffG and WecE reactions. MIDDLE LEFT: LCMS scan of the RffG reaction. MIDDLE RIGHT: Keto-product structure. BOTTOM LEFT: LCMS scan of the WecE reaction. BOTTOM RIGHT: dTDP-Fuc4NH$_2$ structure

Our standard NH2-HPLC analysis was not amenable to liquid chromatograph mass spectrometry (LC-MS) because of the high concentration of buffer required (250 mM ammonium acetate at pH 4.5). Alternatively, an LC-MS method has been developed by the group utilizing a column designed for hydrophilic interaction chromatography (HILIC) to obtain mass spectra of the reaction products. It was found that the RffG product had a mass to charge ratio consistent with the expected 4-keto product, but also had a peak consistent with starting material that was not evident on the amine column. However, previous work on similar enzymes has shown that nucleotide-linked 4-keto sugars may exist in equilibrium as a dihydroxy and keto form in aqueous solutions[25]. This equilibrium could explain the appearance of a mass consistent with starting material, because the dihydroxy form and starting material would have the same mass. Further, in reactions containing WecE, a large retention time change was observed with the RffG product and starting material, consistent with similar enzymes that form an amine product. HILIC-MS data also corroborated that this shift was due to the amination of the RffG product to dTDP-Fuc4NH_2.

Previous work on RffG and WecE had not addressed the importance of the dTDP structure on recognition by these enzymes. dTDP-Glc is an expensive reagent ($50/mg) while UDP-Glc is much more accessible ($2.8/mg). We next tested whether it was necessary to have the dTDP rather than UDP as the structures only differ by a single hydroxyl group and a methyl group. Analysis of reaction mixtures with UDP-Glc as the substrate for RffG indicated that the formation of product was significantly slower with either RffG, WecE or both, demonstrating that the subtle difference in structure did have an appreciable influence on the ability of the enzymes to interact. However, product was formed in these reactions (Figure 13). UDP-Fuc4NH_2 elutes at 2.8 minutes, while dTDP-Fuc4NH_2 elutes at 3.0 minutes Due to the

similarities in retention time shifts, mass was not obtained for the UDP RffG product, however, the mass for UDP-Fuc4NH$_2$ was confirmed via LCMS.

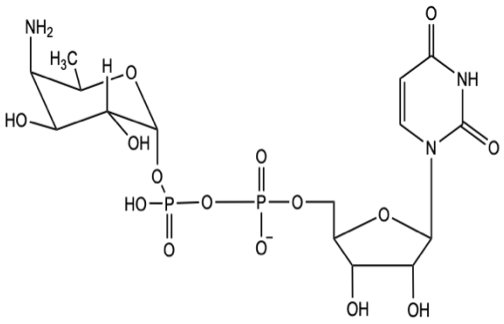

m/z: 548.07 (100.0%), 549.07 (18.2%), 550.07 (4.5%)

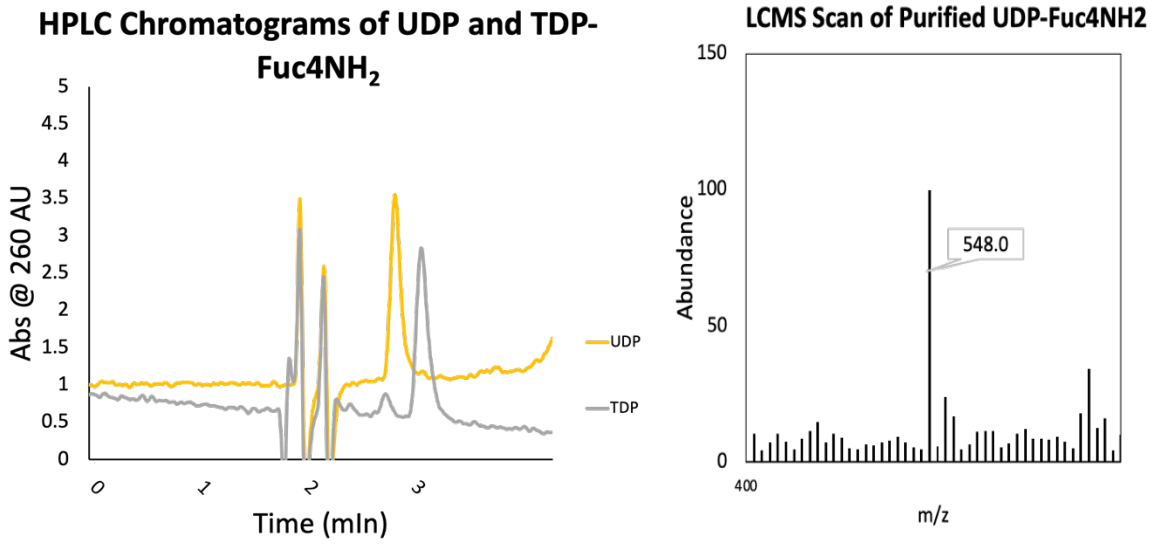

Figure 13: TOP: UDP-Fuc4NH$_2$ structure. BOTTOM LEFT: HPLC Chromatogram displaying the differences in retention time between UDP and dTDP-linked Fcc4NH2. UDP-Fuc4NH2 elutes slightly before thee dTDP sugar, with both around 3 minutes. BOTTOM RIGHT: The LCMS direct injection of the purified UDP-Fuc4NH2.

3.2.2: WecD Enzymatic Reactions

Once the activity of RffG and WecE were confirmed it was then possible to begin the analysis of WecD. To obtain WecD substrate, RffG and WecE product was separated by NH2-HPLC and the major product peak was collected. HPLC buffer was then removed by lyophilization giving a 60% yield of dTDP-Fuc4NH$_2$ relative to input dTDP-Glc. HPLC analysis of WecD reaction mixtures containing dTDP-Fuc4NH$_2$ indicated there was a clear increase in retention time from the control reaction (no WecD) to the WecD reaction (Figure 14), which indicated that dTDP-Fuc4NAc was formed. The identity of the product was further confirmed when the corresponding m/z signal of 588 detected by LCMS (Figure 14).

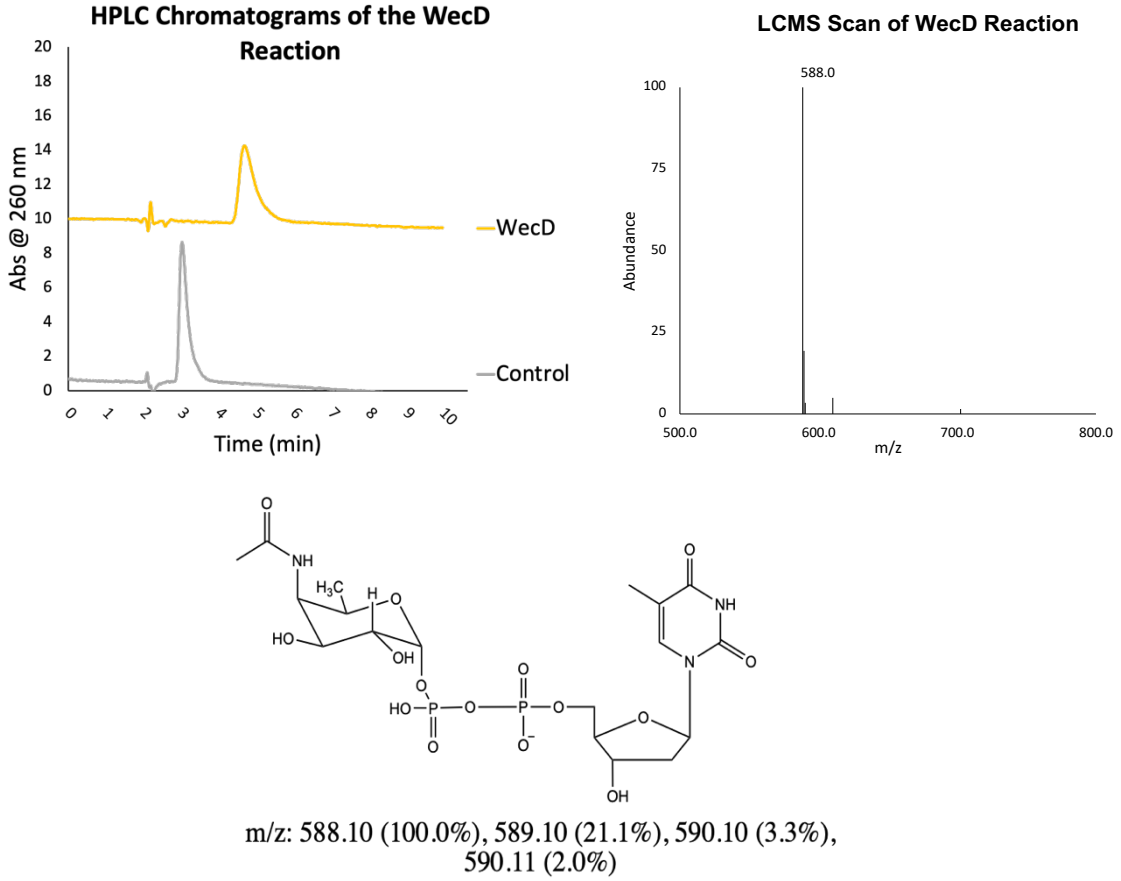

Figure 14: TOP LEFT: HPLC chromatograms of a single WecD reaction. The bottom line represents the control reaction; dTDP-Fuc4NH2 elutes at 3 minutes. The top line indicates the WecD reaction; dTDP-Fuc4NAc elutes at 5 minutes. TOP RIGHT: LCMS SIM data indicates that the mass of the purified product is associated with the correct m/z. BOTTOM: dTDP-Fuc4NAc structure

3.2.3 WecD Kinetic Assays

Michaelis-Menten kinetic analysis provides important information on the ability of enzymes to interact with substrates, the kinetic mechanism of the protein, and serve as a starting point for the *in vitro* investigation of potential inhibitors. While HPLC could be used to measure reaction rates required for kinetic analysis it would require a discontinuous method, in which reactions would have to be quenched at different time points then analyzed. Alternatively, a continuous method that depended on spectroscopic changes would allow us to monitor reactions in real time and could be adapted to a microplate allowing many reactions to be monitored at once. A common method for the continuous monitoring of acetyltransferases utilizes Ellman's reagent[27-28]. Upon the formation of the product dTDP-Fuc4NAc, CoASH is formed as a by-product, which contains a free thiol. Ellman's reagent works by reacting with the free thiol, which in turn results in the formation of a spectroscopic signature at 412 nm (Figure 15). The increase in absorbance at 412 nm and use of a standard curve of known thiol concentrations could then be used to calculate the amount of CoASH, and therefore dTDP-Fuc4NAc, produced over time.

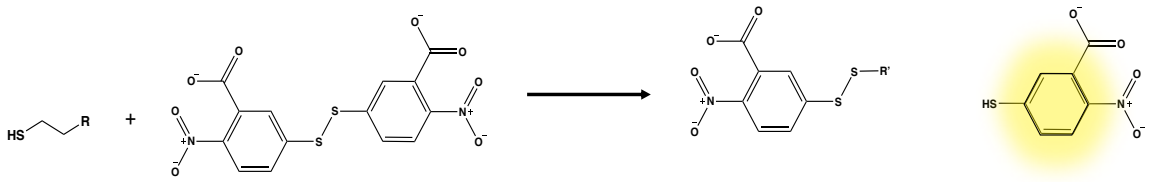

Figure 15: Mechanism of Ellman's Reagent

While the continuous method of analysis was preferred, our initial investigations of the reaction suggested that the use of Ellman's reagent could be problematic. In addition, there are several literature reports suggesting that histidine purification tags could cause problems with the use of Ellman's reagent to monitor protein activity[27-28]. To avoid potential complications of the tagged protein we used the cleaved WecD for the continuous Ellman's assay. First, a standard curve was prepared using β-mercaptoethanol reactions with Ellman's reagent to measure different concentrations of modified thiol (Figure 16). Next, dTDP-Fuc4NH_2 reaction mixtures were prepared with WecD. In the presence of 20 μM dTDP-Fuc4NH_2 and 160 μM AcCoA, 0.1 μg of WecD produced an absorbance of 0.053 after 10 minutes, which based on the standard curve gave 14.7 μM of CoASH. Due to the fact that the WecD reaction produces a 1:1 ratio of dTDP-Fuc4NAc:CoASH, it can be assumed that 14.7 μM of dTDP-Fuc4NAc was produced. The product turnover for 80, 40, 20, and 10 μM AcCoA reactions was 13.4 μM, 10.9 μM, 6.9 μM, 5.2 μM, and 1.25 μM dTDP-Fuc4NAc, respectively. After the reaction had completed on the spectrophotometer, one of the three triplicates was quenched and analyzed by NH2-HPLC to confirm that the Ellman's assay was equivalent to the HPLC assay (Figure 17).

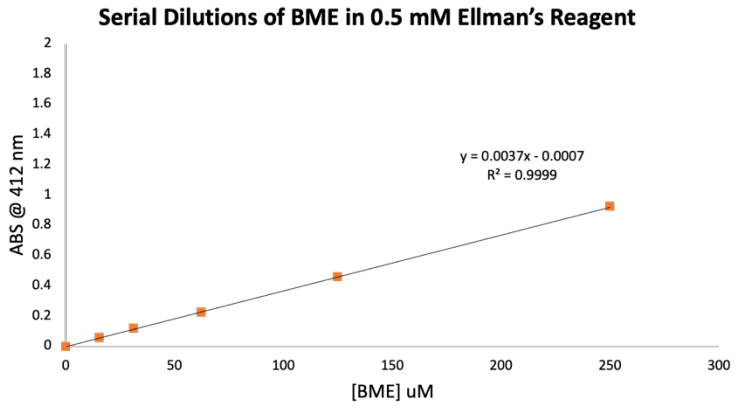

Figure 16: Standard curve of BME used to calculate concentration of dTDP-Fuc4NAc

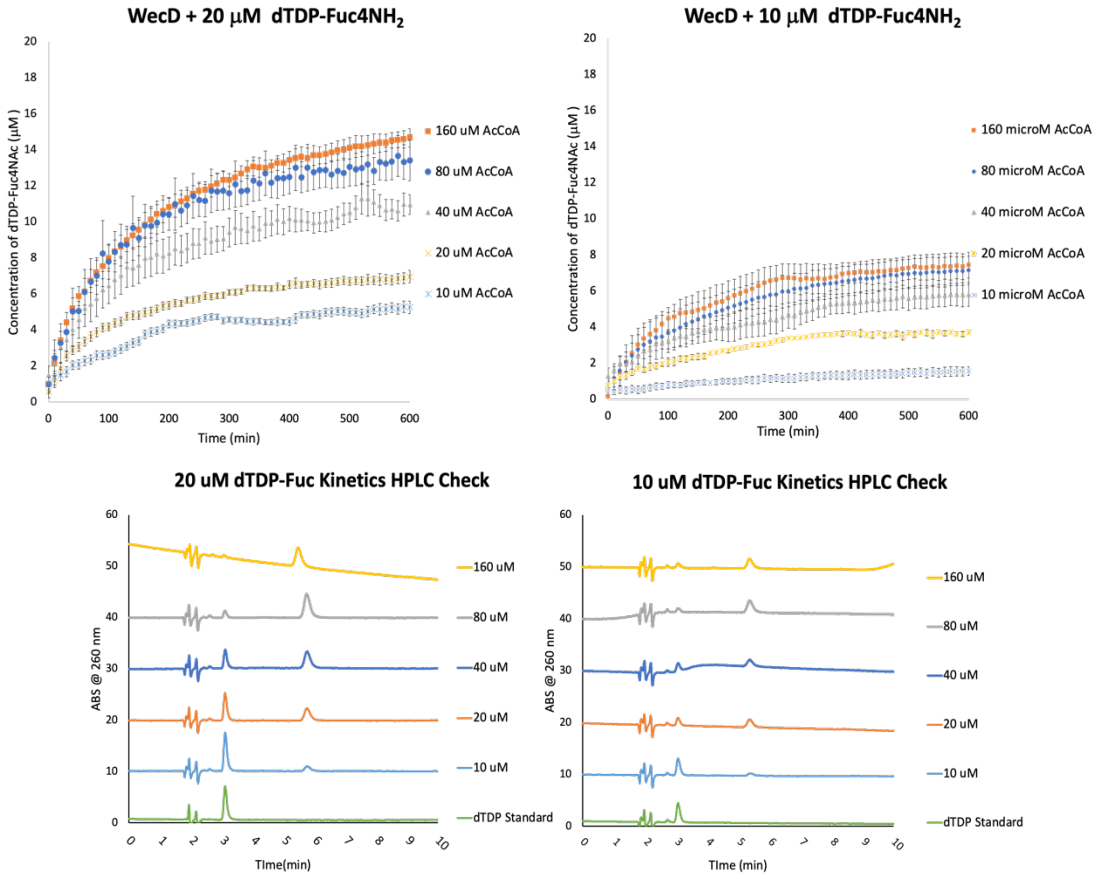

Figure 17: TOP LEFT: Concentration of dTDP-Fuc4NAc that is produced in the presence of 20 μM dTDP-Fuc4NH_2 over 10 minutes. TOP RIGHT: Concentration of dTDP-Fuc4NAc that is produced in the presence of 10 μM dTDP-Fuc4NH_2 over 10 minutes. BOTTOM: HPLC chromatograms of one of the triplicate WecD reactions performed for each concentration of both dTDP-Fuc4NH_2 and AcCoA.

Because WecD uses two substrates, AcCoA and dTDP-Fuc4NH_2, kinetic assays were performed with one substrate held constant (dTDP-Fuc4NH_2), while the other substrate concentration was increased (AcCoA) to obtain apparent kinetic parameters for the enzyme. Initial rates were determined by measuring the slope of the linear phase of each reaction. When the 20 μM dTDP-Fuc4NH_2 data was fit to the Michalis-Menten enzyme model, the apparent K_M

was 86 ± 25 μM, and the apparent k_{cat} was 5 ± 1 s^{-1}. The efficiency of the enzyme, represented by k_{cat}/ K_M, was (5 ± 1) × 10^{-4} $M^{-1} \times s^{-1}$ (Figure 18). When 10 μM dTDP-Fuc4NH_2 was used for the WecD reaction, the apparent Km was 83 ± 50 μM, and the apparent k_{cat} was 2 ± 1 s^{-1}. The k_{cat}/ K_M under these conditions was (3 ± 1) × 10^{-4} $M^{-1} \times s^{-1}$.

The difference in k_{cat}/ K_M at these two concentrations suggests that the enzyme likely does not follow a double-displacement type of kinetic mechanism. However, it is important to note that the large fitting error associated with both the 20 μM and 10 μM dTDP-Fuc4NH_2 is problematic, and additional trials in these concentration ranges need to be performed. However, the suggested kinetic mechanism is consistent with the literature findings for GNATs as well as the data provided from the crystal structure. While some GNATs do undergo a double-

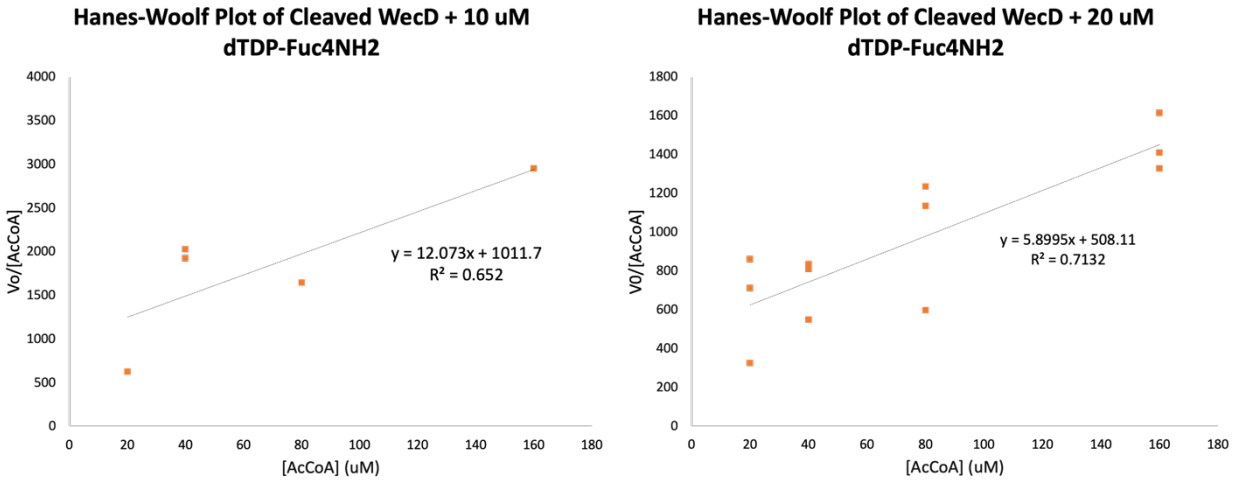

Figure 18: WecD Hanes-Woolf plots

Table 6: Kinetics data for WecD with 10 and 20 μM dTDP-Fuc4NH_2

	10 μM dTDP-Fuc4NH_2
K_M	83 ± 50 μM
k_{cat}	2 ± 1 s^{-1}
k_{cat}/K_M	(3 ± 1) × 10^{-4} $M^{-1} \times s^{-1}$
R	0.65

	20 μM dTDP-Fuc4NH_2
K_M	86 ± 25 μM
k_{cat}	5 ± 1 s^{-1}
k_{cat}/K_M	(5 ± 1) × 10^{-4} $M^{-1} \times s^{-1}$
R	0.71

displacement mechanism, the residues surrounding Acetyl CoA within WecD would be unlikely to accept an acetyl group[26]. As previously mentioned, the primary amine of dTDP-Fuc4NH_2 is thought to act as a nucleophile and attacks the thioester of AcCoA, which points to a ternary enzyme-substrate complex. This is also supported by the fact that AcCoA and dTDP-Fuc4NH_2 enter WecD via opposite sides of the catalytic tunnel and interact with WecD simultaneously[26].

3.2.4. Analysis of the Different Constructs of WecD

It was important to determine whether the purification tag on WecD had an influence on the measured rates. If the tag did influence activity, then it should be observed when comparing the activity of the pET-15b construct cleaved and uncleaved as well as the pET-24a construct. To perform kinetic analysis the pET24a and pET15b data was fit to a Lineweaver-Burke plot, as opposed to the Hanes-Woolf plot (Figure 19). This was because the percent error associated with the Lineweaver-Burke linear equation was less than that of the Hanes-Woolf, and therefore gave a more accurate analysis of the data. The analysis of the two tagged constructs revealed that Km of the pET15b WecD construct appeared to be 41 ± 23 μM, with an apparent k_{cat} of 2 ± 0.5 s^{-1}. This gives a k_{cat}/ K_M of (7 ± 1) × 10^{-4} s^{-1} (Table 7). The pET24a construct had a Km of 32 ± 8 μM and a k_{cat} of 1 ± 0.7 μM/s. The calculated k_{cat}/ K_M value is (3 ± 0.8) × 10^{-4} $s^{=1}$ (Table 7). The kinetic data indicates that there are subtle differences in the three constructs, however due to the large amount of error between the values, more analyses are warranted.

In order to determine if there was a difference in product formation, the initial rates of each of the three constructs of WecD were compared (Table 8). At 160 μM AcCoA, an ANOVA test and a Tukey post-hoc test revealed that the pET15b cleaved and uncleaved enzymes were not statistically different from one another ($p < 0.05$), but the rate of reactions were both

significantly different from that of the pET24a WecD for the first 300 s of the reaction ($p < 0.05$). Additionally, at 20 µM and 40 µM AcCoA, only the cleaved and pET24a WecD reactions were statistically different from one another ($p < 0.05$). For 10 µM and 80 µM AcCoA, the rates of reactions for all three constructs are similar to one another. These data suggest that there is likely little difference in the activity of the three constructs. Additionally, in reactions where dTDP-Fuc4NH$_2$ was left out of the mixture, we observed low background CoASH production from the enzyme suggesting that the tags did not influence the assays (Figure 20). When these reactions were validated using HPLC, the calculated percentage of turnover at each time point fell within 45% of the percentage turnover calculated from the Ellman's reagent assays (Table 9).

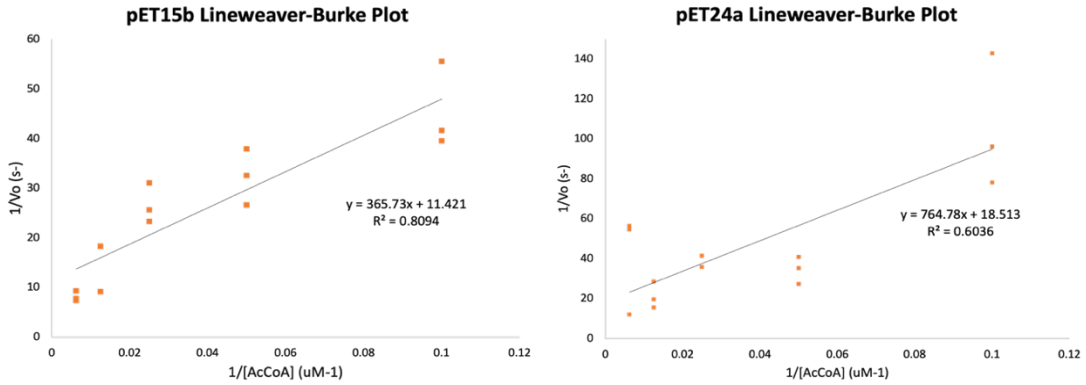

Figure 19: Lineweaver-Burke Plots of kinetic data from pET24a and pET15b WecD constructs

Table 7: Kinetic values from the cleaved, pET15b, and pET24a WecD constructs with 10 µM dTDP-Fuc4NH$_2$

	pET15b
K_M	32 ± 8 µM
k_{cat}	2 ± 0.5 s^{-1}
k_{cat}/K_M	(7 ± 1) × 10^{-4} $M^{-1} \times s^{-1}$
R	0.80

	pET24a
K_M	41 ± 23 µM
k_{cat}	1 ± 0.7 s^{-1}
k_{cat}/K_M	(3 ± 1) × 10^{-4} $M^{-1} \times s^{-1}$
R	0.63

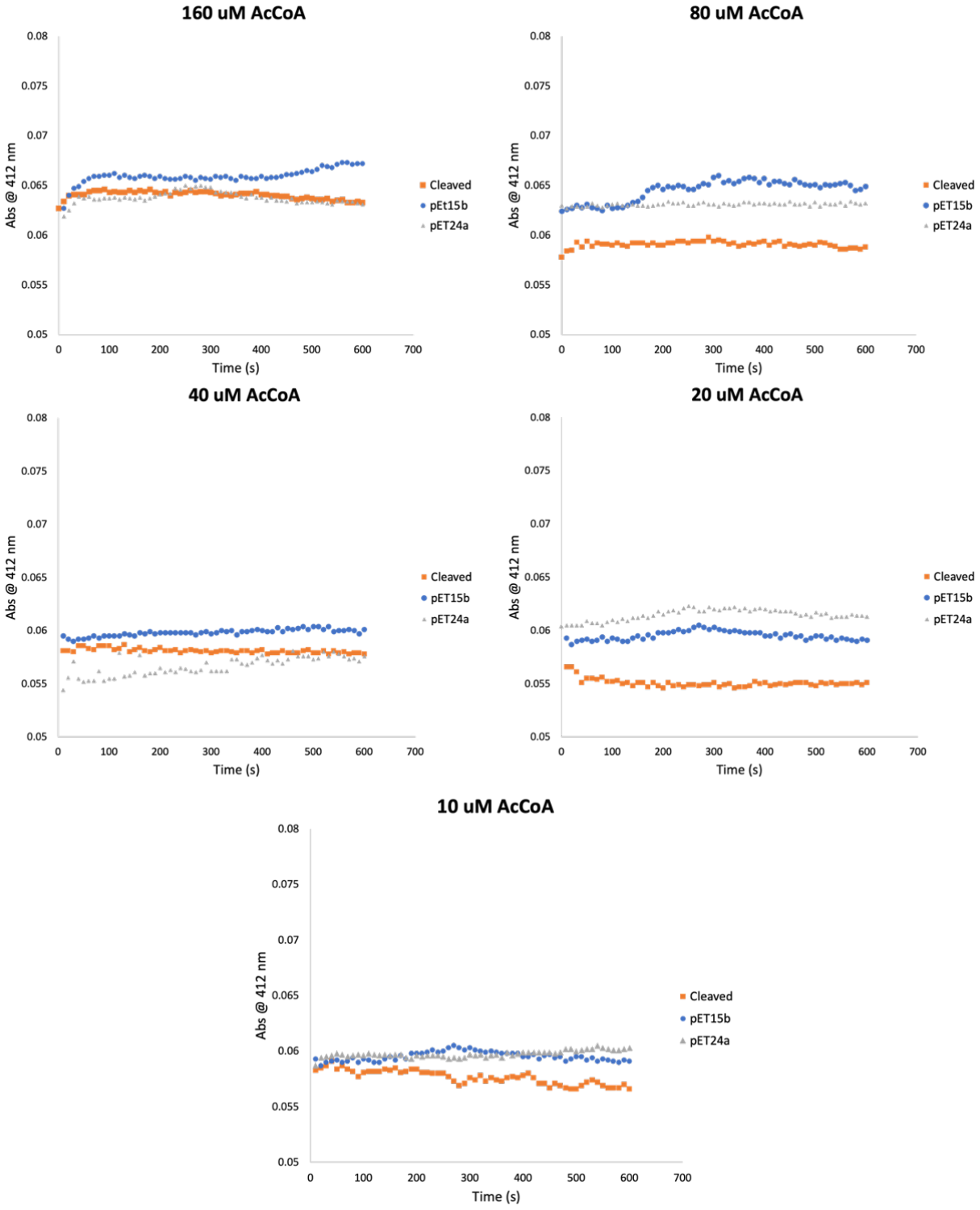

Figure 20: Background absorbance observed in the WecD reactions lacking dTDP-Fuc4NH$_2$

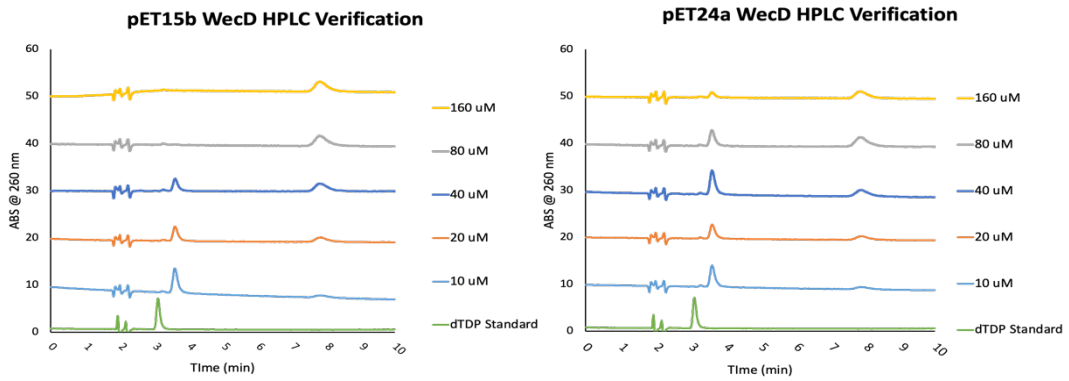

Figure 21: HPLC Verification of dTDP-Fuc4NAc turnover by 10 minutes

Table 9: ANOVA analysis of the rates of reaction of thee 3 constructs of WecD

p-values	10 uM AcCoA	20 uM AcCoA	40 uM AcCoA	80 uM AcCoA	1600 uM AcCoA
ANOVA	0.322	0.037	0.022	0.148	0.039
24a:15b		0.943	0.238		0.034
Cleaved:15b		0.068	0.174		0.408
Cleaved:24a		0.045	0.018		0.89

Table 8: Percent turnover of dTDP-Fuc4NAc by the three constructs of WecD, as measured by both HPLC and ER

[AcCoA]	pET24a		pET15b		Cleaved	
	HPLC	ER	HPLC	ER	HPLC	ER
10	11	12	20	10	6	6
20	23	36	32	40	26	42
40	32	29	55	55	34	67
80	53	61	57	100	67	100
160	54	77	68	92	73	94

3.2.6. WecD Reactions with UDP-Fuc4NH_2

The next question to address was whether WecD activity was influenced by the identity of the nucleotide donor. UDP-Fuc4NH_2 (10 μM) was tested with AcCoA (20 μM) resulting in 47± 1 % turnover by 30 minutes, and 60 ± 0.7 % of the substrate was consumed by 2 hours (Figure 22, Table 10). When compared to a 10 μM dTDP-Fuc4NH_2 reaction, the 30-minute time point resulted in 66 ± 2% and the 60-minute time point resulted in 67 ± 2 %. By two 2 hours, the dTDP-Fuc4NH_2 reaction had converted 70 ± 4 % substrate to product (Table 10). When comparing turnover at the 30-minute dTDP-Fuc4NH_2 to that of the 60-minute time using a paired T-test, it was found that the two points were not significantly different from one another ($p = 0.985$), which indicates that the reaction had plateaued and was no long forming more product. The same outcome can be observed when comparing the 60-minute mark and the 120-mark ($p = 0.46$). The differences in turnover between the 30- and 60-minute UDP-Fuc4NH_2 reaction timepoints were significantly different from one another ($p=0.001$), while the differences between the 60- and 120-minute marks were not ($p=0.09$). These results suggest that some aspect of the UDP structure may cause the WecD reaction to proceed more slowly, and that there is likely some difference in initial rates that should be investigated through kinetic analysis. When dTDP-Fuc4NH_2 interacts with WecD, it is suggested, via computer simulations, that the thymine moiety of dTDP-Fuc4NH_2 forms pi-pi stacking with the aromatic residues Phe122 and Trp126. Some literature suggests that UDP actually forms these bonds less readily than dTDP, which could be the reason that UDP-Fuc4NH_2 was a slower substrate for WecD.

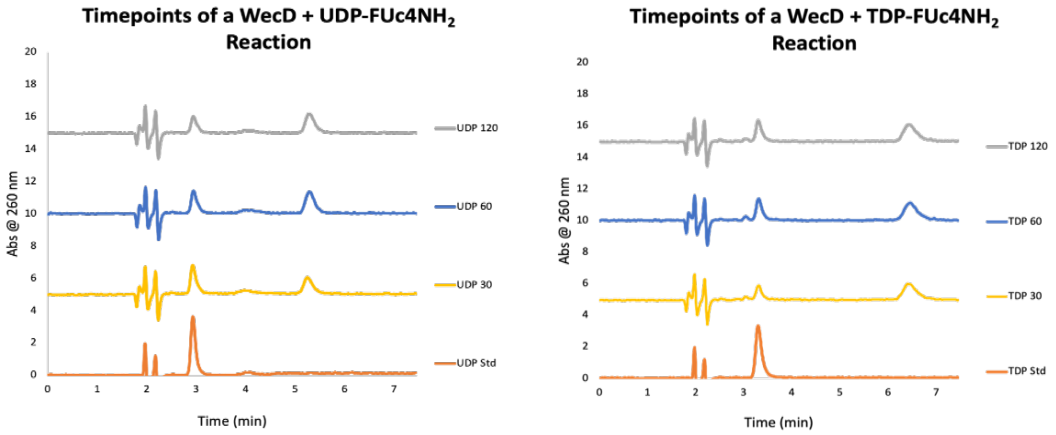

Figure 22: TOP: WecD reaction time point chromatograms with UDP-Fuc4NH2. BOTTOM: WecD reaction time point chromatograms with dTDP-Fuc4NH2

Table 10: The percent turnover of UDP- and dTDP-Fuc4NAc by WecD at 30, 60, and 120 minutes

Time (min)	% $Fuc4NH_2$ Turnover		p-value
	UDP	dTDP	
30	46.68 ± 1.15	65.63 ± 1.78	0.001
60	58.58 ± 0.51	65.68 ± 2.14	0.0032
120	60.47 ± 0.67	69.25 ± 3.8	0.085

3.3: WzyE Reactions

3.3.1: Preparation of the WzyE Substrate

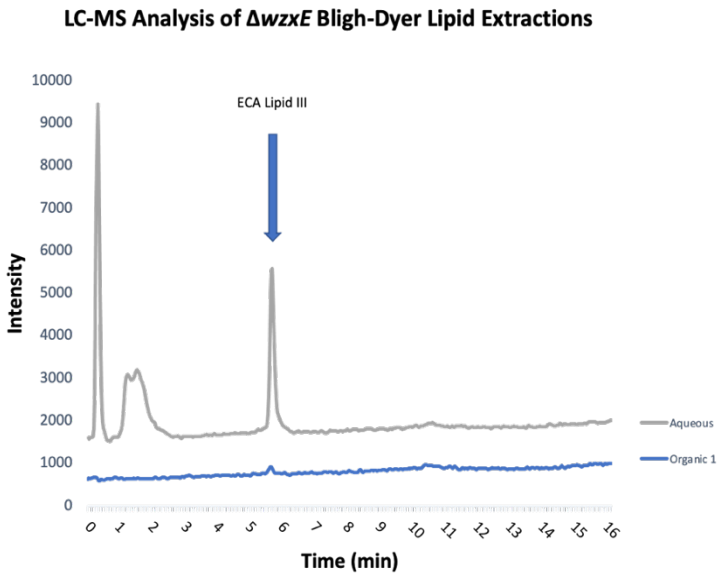

Figure 23: LC-MS Analysis of ΔwzxE Bligh-Dyer lipid extractions. Both SIM chromatograms look for ECA Lipid III. The top chromatogram is the aqueous phase of the lipid extractions, with a clear peak at 5.5 minutes. The bottom chromatogram shows an extremely small peak at the same time, indicating that the majority of Lipid III is in the aqueous phase.

One of the major limitations to working with Wzy polymerases is the lack of access to the protein substrate. Recently, the Troutman group developed a method for obtaining the lipid-linked trisaccharide of ECA for WzyE through the deletion of the ECA flippase gene *wzxE*. *E. coli* strains with *wzxE* deleted from the genome (*ΔwzxE*) and containing a plasmid expressing undecaprenyl pyrophosphate synthase (p*uppS*) to relieve growth defects, were prepared by the Young Lab from the University of Arkansas[7, 25]. After growing the cultures, they were lysed in a 2:1:1 chloroform, methanol, and water. The lysate separated into an aqueous and organic phase that was then analyzed by LC-MS to determine whether ECA Lipid III separated into one or the other. Using SIM detection of the lipid-linked trisaccharide ECA lipid III, we found that the compound was preferentially extracted into the aqueous layer (Figure 23).

3.3.2: WzyE *in vitro* Reactions

A reaction catalyzed by WzyE would be expected to form BPP and a polymer of the trisaccharide linked to BPP as ECA Lipid III decreased. With freshly prepared WzyE membrane fractions and ECA Lipid III we reproducibly observed the disappearance of the lipid-linked starting material by LCMS and did not observe the loss of this material with control membrane fractions that did not contain overexpressed WzyE. However, we did not observe a concomitant increase in BPP when WzyE was present. The amount of BP in the reaction was also consistent between the WzyE 0-time point and the 30- and 60- minute time points, indicating that the amount of cell lysate injected was consistent between the samples, and that the BPP was likely not being recycled to BP. Previous work in our group has suggested that BPP is more difficult to detect by LCMS than BP and ECA Lipid III, highlighting one major weakness in using LCMS for these types of reactions. It is commonly understood that different compounds ionize to different degrees and very similar compounds may have very different limits of detection.

We next tested whether ECA Lipid III decreased over time relative to control reactions (Figure 25, Table 9). Samples of the WzyE reactions were tested at 30 minutes and one hour and examined for the presence of ECA Lipid III, BPP, and BP (Figure 24, Table 11). In these analyses the ECA Lipid III did decrease in the presence of WzyE, but we also observed changes in the levels of ECA Lipid III in control reactions. However, it should be noted that the control reactions likely still contain basal levels of WzyE expressed from the genomic DNA. It is also problematic to inject consistent levels of membrane containing lysate material for HPLC analysis, as membrane containing solutions can be heterogenous even when they appear not to be. To control for this, we analyzed the ratio of BP to Lipid III in these reactions, as BP levels were not expected to change over time. Due to the fact that the control reaction lacked WzyE,

and the ECA Lipid III was extracted from the aqueous phase of the Bligh-Dyer lipid extraction (whereas BP would have remained in the organic phase), there was not a detectable amount of BP in the control reaction to take into account. When controlling for injection using BP as an internal standard, the ratio of Lipid III to BP continuously decreased. This indicates that the amount of Lipid III was decreases as compared to the consistent BP levels.

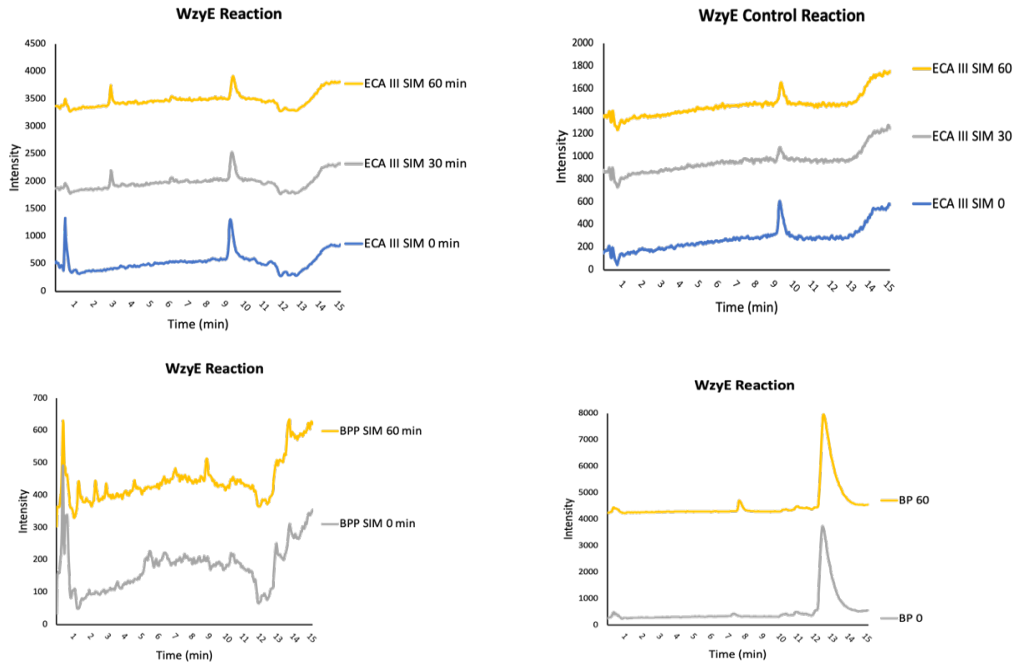

Figure 24: LCMS Analysis of WzyE reactions. TOP LEFT: ECA Lipid III SIM peaks from a WzyE reaction. TOP RIGHT: ECA Lipid III SIM peaks from the control reaction that lacked WzyE. BOTTOM LEFT: BPP SIM peaks from the WzyE reaction. BOTTOM RIGHT: BP SIM peaks from a

Table 11: The percentage that the ECA Lipid III peak decreases over time

Time Point	% of ECA Lipid III Peak Lost from 0		ECA/BP
	WzyE Reaction	Control	WzyE Reaction
0	0	0	.103
30	37.6%	57%	0.056
60	47.8%	19.9%	0.048

CHAPTER 4: CONCLUSIONS AND FUTURE WORK

4.1: WecD Characterization

In this work, I focused on studying the acetyltransferase WecD, which is responsible for synthesizing the final monosaccharide added to the ECA trisaccharide repeat unit. In addition to the ECA being connected to membrane permeability in the bacterial family *Enterobacteriaceae*, there is also evidence of its involvement in virulence of *Salmonella.* It is hypothesized that an inhibitor of WecD could act as an anti-virulence medication against *Salmonella* and potentially other *Enterobacteriaceae*. Because the ECA is not required for bacterial survival, making an anti-virulence medication could be effective to combat resistance because the bacteria face less selective pressure to develop resistance.

After using RffG and WecE to form the WecD starting material dTDP-Fuc4NH_2, I was able to confirm that all three constructs of the WecD protein were functional. Early investigation into protocols used for other enzymes in the GNAT enzymatic family suggested that the 6-His tag commonly used to purify proteins could be problematic for using Ellman's Reagent assays. To this end a new construct of WecD was prepared in my work that allowed for the cleavage of the purification tag. Surprisingly, I found that the activity of WecD varied little between C-terminal and N-terminal hexahistidine tags, and there was little difference in activity when the tag was removed. What was clear from this analysis was that there was no background detected from the tagged WecD proteins, suggesting that it may not be necessary to remove tags for analysis using Ellman's reagent.

UDP and dTDP are often considered to be interchangeable in glycan assembly pathways, and it was of interest to determine whether this was the case for sugar modifying enzymes needed to build rare bacterial sugars. When UDP-Fuc4NH_2 was tested as a substrate, we found

that there was a difference in the activity of WecD, where at 30-minutes and 60-minutes significantly less product was formed when UDP-FucNH_2 was used as a substrate rather than dTDP-Fuc4NH_2. The difference in activity appeared to be kinetic rather than thermodynamic as the total product formation was similar between the two substrates after two hours.

The differences between UDP and dTDP may be due to the suggested interactions between the thymine moiety of dTDP-Fuc4NH_2 and the WecD residues Phe122 and Trp126[26]. Literature has suggested that thymine forms parallel stacks with Trp more readily than uridine[33]. Performing site-directed mutagenesis on both Phe122 and Trp126 may alleviate the specificity of the protein for dTDP and enhance activity with UDP. Leucine is the largest non-polar residue, so changing these residues to leucine would likely cause the least effects on the overall WecD structure. If dTDP-Fuc4NH_2 does form parallel stacks with Phe122 and Trp126, then turnover of dTDP-Fuc4NAc should not occur. Additionally, a Trp122Phe mutant could also be made to test if UDP-Fuc4NH_2 works more effectively when tryptophan is replaced.

4.2: *In vitro* Polymerization of the ECA

In vitro polymerization of lipid-linked oligosaccharides is a major challenge in bacterial glycoscience. While attempting to use the polymerase WzyE, we were able to obtain data that suggested that the starting lipid-linked trisaccharide of ECA was being consumed in membrane preparations containing overexpressed WzyE. When incubating WzyE and Lipid III together, we were able to see a decrease in the amount of ECA Lipid III on the LCMS which was greater than that of the control reaction. However, we expected to observe an increase of BPP or BP but did not detect either increasing. The decrease in ECA lipid III also was progressive over time. However, the lack of detectable BPP formation is concerning. Future studies on WzyE should utilize the *in vitro* synthesis of the Lipid III on a fluorescent analogue of BP, as we've used

before for other pathways[13]. With the fluorescent tag it will be significantly easier to determine whether polymer is being formed on the tagged molecule, and identifying fluorescent BPP, BP or even bactoprenol would be more straightforward than using mass detection.

REFERENCES

1. Mao, Y.; Doyle, M. P.; Chen, J., Role of colanic acid exopolysaccharide in the survival of enterohaemorrhagic Escherichia coli O157:H7 in simulated gastrointestinal fluids. *Lett Appl Microbiol* **2006,** *42* (6), 642-7.

2. Senchenkova, S. N.; Shashkov, A. S.; Shneider, M. M.; Arbatsky, N. P.; Popova, A. V.; Miroshnikov, K. A.; Volozhantsev, N. V.; Knirel, Y. A., Structure of the capsular polysaccharide of Acinetobacter baumannii ACICU containing di-N-acetylpseudaminic acid. *Carbohydr Res* **2014,** *391*, 89-92.

3. Wilson, R. P.; Winter, S. E.; Spees, A. M.; Winter, M. G.; Nishimori, J. H.; Sanchez, J. F.; Nuccio, S. P.; Crawford, R. W.; Tukel, C.; Baumler, A. J., The Vi capsular polysaccharide prevents complement receptor 3-mediated clearance of Salmonella enterica serotype Typhi. *Infect Immun* **2011,** *79* (2), 830-7.

4. Hahn, M. M.; Gunn, J. S., Salmonella Extracellular Polymeric Substances Modulate Innate Phagocyte Activity and Enhance Tolerance of Biofilm-Associated Bacteria to Oxidative Stress. *Microorganisms* **2020,** *8* (2).

5. 2019 Antibiotic Resistance Threats Report. https://www.cdc.gov/drugresistance/biggest-threats.html (accessed August 1).

6. Antibitoic Restance The Global Threat. https://www.cdc.gov/globalhealth/infographics/antibiotic-resistance/antibiotic_resistance_global_threat.htm (accessed 20 May).

7. Jorgenson, M. A.; Kannan, S.; Laubacher, M. E.; Young, K. D., Dead-end intermediates in the enterobacterial common antigen pathway induce morphological defects in Escherichia coli by competing for undecaprenyl phosphate. *Molecular Microbiology* **2016,** *100*, 1-14.

8. Avci, F. Y.; Li, X.; Tsuji, M.; Kasper, D. L., A mechanism for glycoconjugate vaccine activation of the adaptive immune system and its implications for vaccine design. *Nature Medicine* **2011,** *17*, 1602-1610.

9. Bridge, D. R.; Whitmire, J. M.; Gilbreath, J. J.; Metcalf, E. S.; Merrell, D. S., An enterobacterial common antigen mutant of Salmonella enterica serovar Typhimurium as a vaccine candidate. *Int J Med Microbiol* **2015,** *305* (6), 511-22.

10. Ma, Y.; Li, X.; Li, W.; Liu, Z., Glycan-Imprinted Magnetic Nanoparticle-Based SELEX for Efficient Screening of Glycoprotein-Binding Aptamers. *ACS Appl Mater Interfaces* **2018,** *10* (47), 40918-40926.

11. Lujan, D. K.; Stanziale, J. A.; Mostafavi, A. Z.; Sharma, S.; Troutman, J. M., Chemoenzymatic synthesis of an isoprenoid phosphate tool for the analysis of complex bacterial oligosaccharide biosynthesis. *Carbohydr Res* **2012,** *359*, 44-53.

12. Barr, K.; Nunes-Edwards, P.; Rick, P. D., In vitro synthesis of a lipid-linked trisaccharide involved in synthesis of enterobacterial common antigen. *J Bacteriol* **1989,** *171* (3), 1326-32.

13. Reid, A. J.; Scarbrough, B. A.; Williams, T. C.; Gates, C. E.; Eade, C. R.; Troutman, J. M., General Utilization of Fluorescent Polyisoprenoids with Sugar Selective Phosphoglycosyltransferases. *Biochemistry* **2020,** *59*, 615-626.

14. Ramos-Morales, F.; Prieto, A.; Beuzone, C.; Holden, D.; Cassadesus, J., Role for Salmonella enterica Enterobacterial Common Antigen in Bile Resistance and Virulence. *Journal of Bacteriology* **2003,** *185*, 5328-5332.

15. Gozdziewicz, T. K.; Lugowski, C.; Lukasiewicz, J., First evidence for a covalent linkage between enterobacterial common antigen and lipopolysaccharide in Shigella sonnei phase II ECA(LPS) (vol 289, pg 2745, 2017). *Journal of Biological Chemistry* **2018,** *293* (29), 11652-11653.

16. Rai, A. K.; Mitchell, A. M., Enterobacterial Common Antigen: Synthesis and Function of an Enigmatic Molecule. *mBio* **2020,** *11* (4).

17. Erbel, P. J. A.; Barr, K.; Gao, N.; Gerwig, G. J.; RIck, P. D.; Garder, K. H., Identification and Biosynthesis of Cyclic Enterobacterial Common Antigen in Escherichia coli. *Journal of Bacteriology* **2002,** *185*, 1995-2004.

18. Kunin, C. M., Separation, Characterization, and Biological Significance of a Common Antigen in Enterobacteriaceae. *J Exp Med* **1963,** *118*, 565-86.

19. Wang, K. C.; Huang, C. H.; Chang, P. R.; Huang, M. T.; Fang, S. B., Role of wzxE in Salmonella Typhimurium lipopolysaccharide biosynthesis and interleukin-8 secretion regulation in human intestinal epithelial cells. *Microbiol Res* **2020,** *238*, 126502.

20. Mitchell, A. M.; Srikumar, T.; Silhavy, T. J., Cyclic Enterobacterial Common Antigen Maintains the Outer Membrane Permeability Barrier of Escherichia coli in a Manner Controlled by YhdP. *American Society for Microbiology* **2018,** *9* (4), 1-16.

21. Westfall, C. S., An "Uncommon" Role for Cyclic Enterobacterial Common Antigen in Maintaining Outer Membrane Integrity. *American Society for Microbiology* **2018,** *9* (5), 1-3.

22. Krasny, S. A.; Gorzynski, E. A., Immunological Cross-Reaction between Enterobacterial Common Antigen and Rat-Tissue. *Immunopharmacology* **1979,** *2* (1), 1-8.

23. Lugowski, C.; Kulakowska, M.; Romanowska, E., Enterobacterial Common Antigen-Tetanus Toxoid Conjugate as Immunogen. *American Society for Microbiology* **1983,** *42* (3), 1086-1091.

24. Danese, P. N.; Oliver, G. R.; Barr, K.; Bowman, G. D.; RIck, P. D.; Silhavy, T., Accumulation of the Enterobacterial Common Antigen Lipid II Biosynthetic Intermediate Stimulates degP Transcription in Escherichia coli. *Journal of Bacteriology* **1998,** *180* (2), 5875-5884.

25. Eade, C. R.; Wallen, T. W.; Gates, C. E.; Oliverio, C. L.; Scarbrough, B. A.; Reid, A. J.; Jorgenson, M. A.; Young, K. D.; Troutman, J. M., Making the Enterobacterial Common Antigen Glycan and Measuring Its Substrate Sequestration. *ACS Chem Biol* **2021**.

26. Hung, M. N.; Rangarajan, E.; Munger, C.; Nadeau, G.; Sulea, T.; Matte, A., Crystal Structure of TDP-Fucosamine Acetyltransferase (WecD) from Escherichia coli, and Enzyme Required for Enterobacterial Common Antigen Synthesis. *Journal of Bacteriology* **2006,** *188*, 5606-5617.

27. Kuhn, M. L.; Majorek, K. A.; Minor, W.; Anderson, W. F., Broad-substrate screen as a tool to identifysubstrates for bacterial Gcn5-related N-acetyltransferases with unknown substrate specificity. *Protein Science* **2012,** *22*, 222-230.

28. Majorek, K. A.; Kuhn, M. L.; Chruszcz, M.; Anderson, W. F.; Minor, W., Structural, functional, and inhibition studies of a Gcn5-related N-acetyltransferase (GNAT) superfamily protein PA4794: a new C-terminal lysine protein acetyltransferase from pseudomonas aeruginosa. *J Biol Chem* **2013,** *288* (42), 30223-35.

29. Merino, S.; Gonzalez, V.; Tomás, J. M., The first sugar of the repeat units is essential for the Wzy polymerase activity and elongation of the O-antigen lipopolysaccharide. *Future Microbiology* **2016,** *11* (7), 903-918.

30. Woodward, R.; Yi, W.; Li, L.; Zhao, G.; Eguchi, H.; Perali, R. S.; Guo, H.; Song, J. K.; Motari, W.; Cai, L.; Kelleher, P.; Liu, X.; Han, W.; ZHang, W.; Ding, Y.; Li, M.; Wang, P. G., In Vitro Bacterial Polysaccharide Biosynthesis: Defining the Functions of Wzy and Wzz. *Nat Chem Biol* **2010,** *6* (6), 418-423.

31. Liu, L.; Zha, J.; DiGiandomenico, A.; McAllister, D.; Stover, C. K.; Wang, Q.; Boons, G. J., Synthetic Enterobacterial Common Antigen (ECA) for the Development of a Universal Immunotherapy for Drug-Resistant Enterobacteriaceae. *Angew Chem Int Ed Engl* **2015,** *54* (37), 10953-7.

32. Rath, A.; Glibowicka, M.; Nadeau, V. G.; Chen, G.; Deber, C. M., Detergent binding explains anomalous SDS-PAGE migration of membrane proteins. *Proc Natl Acad Sci U S A* **2009,** *106* (6), 1760-5.

33. Cysewski, P., A post-SCF complete basis set study on the recognition patterns of uracil and cytosine by aromatic and p–aromatic stacking interactions with amino acid residues. *Physical Chemistry Physical Chemists* **2008,** *10*, 2636-2645.